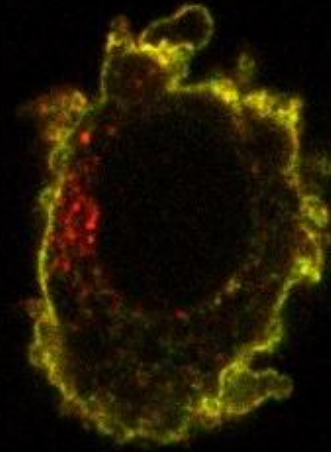


A study of human CD11c as a potential receptor for targeted vaccines



Master Thesis

By Fie Søndergaard

Medicine with Industrial Specialization, Biomedicine

Laboratory of Immunology, Department of Health Science and Technology,

Aalborg University, Denmark

29th of May 2015

Title: A study of human CD11c as a potential receptor for targeted vaccines

Project period: 3rd of September 2014 – 29th of May 2015

Project group: 1009

Author: Fie Søndergaard, 20102938

Supervisor: Ralf Agger

Co-supervisor: Lotte Hatting Pugholm

Pages: 61 (appendix: 57)

Finished: 29th of May 2015

Abstract:

Dendritic cells have been studied intensely for a few decades for their excellent antigen-presenting capabilities, and lately the focus has been on the idea of utilizing them for therapeutic cancer vaccines. Previous studies have shown great potential of using the CD11c molecule as a target on the dendritic cells. However, studies are focusing on the murine model and not much is known about the potential of targeting CD11c in human models.

The aim of the project was to investigate how CD11c is distributed in the blood, how 2 CD11c antibody clones affect dendritic cell maturation and if they are internalized by the dendritic cells.

CD11c distribution was analyzed by flow cytometry, dendritic cell maturation by flow cytometry and microscopy and CD11c internalization by confocal microscopy and flow cytometry.

Results showed that CD11c was expressed by both dendritic cells and monocytes in the blood. Neither of the CD11c antibody clones induced maturation of dendritic cells. CD11c antibody clones was internalized by dendritic cells; 12,63 % and 16,27 % internalization was observed.

Acknowledgements

The research described in this thesis was carried out in the Laboratory of Immunology at Aalborg University from September 2014 to May 2015.

I am using this opportunity to express my gratitude to everyone who supported me throughout the course of my Masters project. First, I would like to thank my supervisor Ralf Agger for making this project possible with funding, keeping the project on track and always giving great advice and guidance. Second, I would like to thank my co-supervisor Lotte Hatting Pugholm for refreshing new ideas and feedback concerning laboratory procedures and project in general. Third, I would also like to thank laboratory technician Brita Holst Jensen for all the help and practical advice in the laboratory and for being available and wanting to help even in inconvenient times. I would also like to thank fellow Master student Esben Christensen, assistant professors Rasmus Foldbjerg and Emil Kofod-Olsen for all their support, advice and help they provided throughout the project period. Furthermore, I would like to thank colleagues who donated blood for the times I could not provide it myself, Aalborg Sygehus for providing a portion of the antibodies used in the experiments and the Laboratory for Medical Mass Spectrometry and the Laboratory for Stem Cell Research at Aalborg University for providing some of the materials used.

Lastly, I would thank my family and friends for supporting me throughout the project which helped me stay focused and motivated to make it to completion.

Thank you,

Fie

Contents

Acknowledgements	1
1 Introduction.....	4
1.1 Dendritic cells	4
1.1.1 Dendritic cell functions	5
1.1.4 Dendritic cell subpopulations	8
1.1.5 DC surface markers	11
1.1.6 Human versus murine dendritic cells	12
1.2 Dendritic cell vaccines	13
1.3 CD11c – a candidate target for future targeted vaccines.....	14
1.4 Flow cytometry	17
1.5 Confocal microscopy	19
2 Study aim.....	20
3 Materials and methods	21
3.1 Isolation of PBMCs	21
3.2 Monocyte isolation	21
3.3 DC differentiation.....	22
3.4 Antibodies.....	22
3.5 Flow cytometric analysis	23
3.6 Confocal microscopy	23
3.7 CD11c distribution assay	24
3.8 Maturation assay	24
3.9 Internalization assay.....	24
4 Results	25
4.1 Gating	25
4.2 Controls	26
4.2.1 Isotype control	26
4.2.2 Doublet control	27
4.2.3 Lymphocyte control.....	28
4.2.4 Monocyte control.....	29
4.3 Pilot experiments	30
4.3.1 Separation of immature and mature populations	30
4.3.2 Morphology of immature and mature moDCs.....	31

4.3.3 Optimization of isolation kit.....	32
4.3.4 Optimization of columns.....	34
4.4 CD11c distribution.....	35
4.4.1 CD11c distribution in whole blood	35
4.4.2 CD11c distribution in PBMCs	36
4.4.3 CD11c distribution in PBMCs analyzed on a cell sorter	37
4.4.4 CD11c distribution in negative isolated monocytes	38
4.4.5 CD11c distribution in positive isolated monocytes	39
4.5 Maturation.....	40
4.5.1 Maturation by CD11c antibody clone 3.9	40
4.5.2 Maturation by CD11c antibody clone BU15	41
4.6 Internalization of CD11c	42
4.6.1 Confocal microscopy	42
4.6.2 Flow cytometric analysis.....	50
4.7 CD11c as an antigen target.....	51
4.7.1 Presentation of a CD11c mouse monoclonal antibody to a mouse immunoglobulin specific T cell clone.....	51
5 Discussion	52
5.1 Flow cytometry controls.....	52
5.2 Confocal microscopy controls.....	52
5.3 Pilot experiments	53
5.4 CD11c distribution.....	53
5.5 Maturation.....	54
5.6 Internalization.....	54
5.7 Perspectives.....	54
6 Conclusion	56
7 Bibliography.....	57
8 Appendix	62

1 Introduction

In the recent years, dendritic cells (DCs) have been studied intensely for their antigen presenting properties and the possibility of using them as a vaccine gateway. DCs have a strong capability of activating both T- and B-cells by presenting antigens and are therefore an ideal targets for immunomodulation by vaccination (1,2).

Already developed and FDA approved is the PROVENGE vaccine, a vaccine meant to treat prostate cancer by stimulating autologous DCs *ex vivo* with a fusion protein that combines the prostate cancer specific prostate acid phosphatase (PAP) with granulocyte-macrophage colony-stimulating factor (GM-CSF). DCs are isolated from patients, and after approximately 40 hours of incubation with the fusion protein, the cells are purified and administered back into the patient to elicit an immune response to PAP expressed on the cancerous cells. Results from the phase III clinical trial reported good results with low adverse effects and a 4.1 month prolonged median survival compared to the placebo control group that had a median survival of 21.7 months (3,4).

Overall, PROVENGE represents a major achievement in the development of effective vaccines against cancer and marks the start of a new era in vaccine technology by the use of DCs.

Additionally, many researchers have performed both *in vitro* and *in vivo* experiments in mice and some *in vitro* in humans, targeting different molecules and receptors on DCs to trigger an immune response against cancer-specific antigens. Generally, the success rate is very high and the possibility of translating the murine results to human models looks promising. Several murine studies conclude that CD11c, an integrin primarily expressed on DCs in mice, could be an optimal molecule to target in order to obtain efficient antigen uptake and presentation (5-7).

Currently, phase 1 and 2 clinical trials are recruiting patients for the study of side effects and best dose of a vaccine that targets CD205 on DCs, meant to treat ovarian, fallopian tube and other primary peritoneal cancers in remission along with a different version still targeting CD205 meant to treat myeloid leukemia (8).

1.1 Dendritic cells

DCs were first identified by Steinman and Cohn in 1973 by harvesting and analyzing adherent cells from the mouse spleen and lymph nodes. They described the cell as one with a distinct morphology:

“The cytoplasm of this large cell is arranged in pseudopods of varying length, width, form, and number, resulting in a variety of cell shapes ranging from bipolar elongate cells to elaborate, stellate or dendritic ones”, see figure 1.1. They concluded that the term “dendritic cell” was appropriate for this novel cell type (9).

DCs originate from dedicated DC stem cells but some are differentiated from monocytes. In culture, it is possible to differentiate bone marrow progenitor cells or circulating blood monocytes into DCs by culturing them in a cytokine cocktail consisting of GM-CSF and interleukin-4 (IL-4) (10).

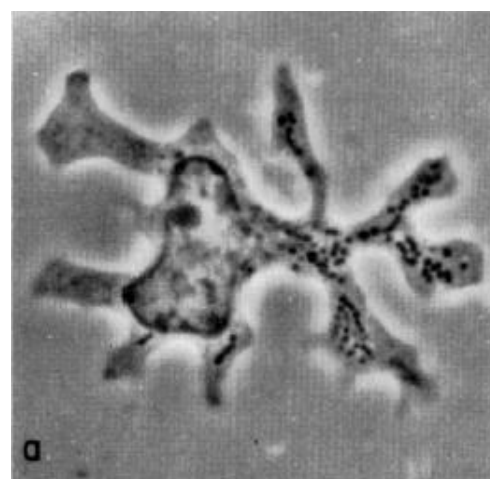


Figure 1.1. First visualization of a dendritic cell. Phase contrast micrograph of dendritic cells isolated from mouse spleen fixed in glutaraldehyde. X 4500. Reprint from (9).

1.1.1 Dendritic cell functions

DCs play a very important role in the immune system by inducing immune responses to foreign antigens while maintaining a tolerance to self antigens. DCs constantly sample the environment for possible intruders. They act as antigen presenting cells (APCs) in the immune system by capturing, processing and presenting antigens to T- and B-cells. DCs make up the important link between the innate immunity and the antigen specific adaptive immunity (5,10,11).

Although the number of blood circulating DCs is relatively low – less than 1 % is found in peripheral blood mononuclear cells (PBMCs) (12) – they are extremely effective in their role as APCs when matured and located in the lymphoid organs. One DC can interact with up to 5000 T-cells in an hour, and thereby trigger a rapid and substantial immune response to an encountered antigen (13). Unique in their ability to induce primary immune responses, they aid in the establishment of immunological memory (5,11).

Circulating DCs acts as sentinels to scout out antigens to internalize and present to T- and B-cells. Depending on the nature of the antigen, DCs may mature upon antigen encounter and subsequently migrate to nearby lymphoid organs where they present the antigens to effector cells (11,14). DCs have several types of surface receptors to recognize damaged cell- or danger associated molecular patterns (DAMPs) and pathogen-associated molecular patterns (PAMPs). Byproducts released from injured cells can actively form DAMPs, for example DNA, RNA and heat shock proteins that are oxidized and denatured. PAMPs are molecules associated with pathogenic microbial intruders and are recognized by the immune system with pattern recognition receptors (PRRs). Some of the best described PRRs are toll-like receptors (TLRs) and C-type lectin receptors (CLRs). For example, TLR4 recognizes the PAMP lipopolysaccharide (LPS) and the mannose-receptor is a well-known CLR that recognizes and binds to mannose units on microbes (13,15). DCs are able to capture antigens by different pathways; macropinocytosis, receptor-mediated endocytosis (eg. C-type lectin DEC-205) and phagocytosis (which is mostly used to internalize particles such as apoptotic and necrotic cell fragments, virus and bacteria) (11).

DCs take up antigens and present them on major histocompatibility complex (MHC) I and II. An antigen (self or foreign) is broken down into peptides in a proteasome. Transport peptides then transports the peptides to the endoplasmatic reticulum to fuse with MHC I and is then transported to the cell membrane for presentation. DCs are able to cross-present foreign antigens on MHC I whereas other cells commonly express only self-antigens on MHC I (10).

The MHC II pathway is slightly longer; an antigen is taken up by the cell and encapsulated in a phagosome that fuses with lysosomes containing enzymes that degrades antigens into peptides. The endosome-lysosome compartment will then fuse with a MHC II containing vesicle that was newly synthesized in the endoplasmatic reticulum and exported through the golgi apparatus. The peptides formed from the antigen are loaded by releasing the class-II associated invariant chain peptide (CLIP) from the peptide-binding domain on MHC II and replacing it with the peptide. The newly formed antigen peptide-MHC II complex is then transported to the cell membrane for presentation (10,16).

Upon encounter and uptake of an antigen containing PAMPs, the DC transforms from the immature state into a mature state with several changes that enables the DC to stimulate native T-cells. The DC loses some of its endocytic and phagocytic receptors, upregulates surface expression of MHC II, CD83 and co-stimulatory molecules CD40, CD80 and CD86, changes internal compartments and overall morphology

(11,13). Morphological changes include cytoskeleton reorganization and loss of adhesive receptors which results in higher motility for the DC to migrate to nearby lymphoid organs (11). Some of the most important chemokine changes that affect the motility are the down regulation of CCR1, CCR2, CCR5 and CCR6 that allow for the DCs to enter into peripheral tissues. CCR7 is upregulated by TLR-signaling and binds to CCL19 and CCL21. CCL21 is expressed in the T-cell zone in secondary lymphoid tissues and helps attract DCs that are expressing CCR7 (10,11,17,17).

After homing to nearby secondary lymphoid tissues, the DC will initiate an immune response by interacting with T-cells and either activating them or inducing T-cell anergy. Immature and semi-mature DCs can migrate to secondary lymphoid tissues in their steady state with self-antigens and interact with T-cells leading to self-tolerance by T-cell anergy or generation of regulatory T-cells (13). An illustration of the different outcomes of T-cells depending on danger signals or tolerance stimuli from the DCs can be found in figure 1.2.

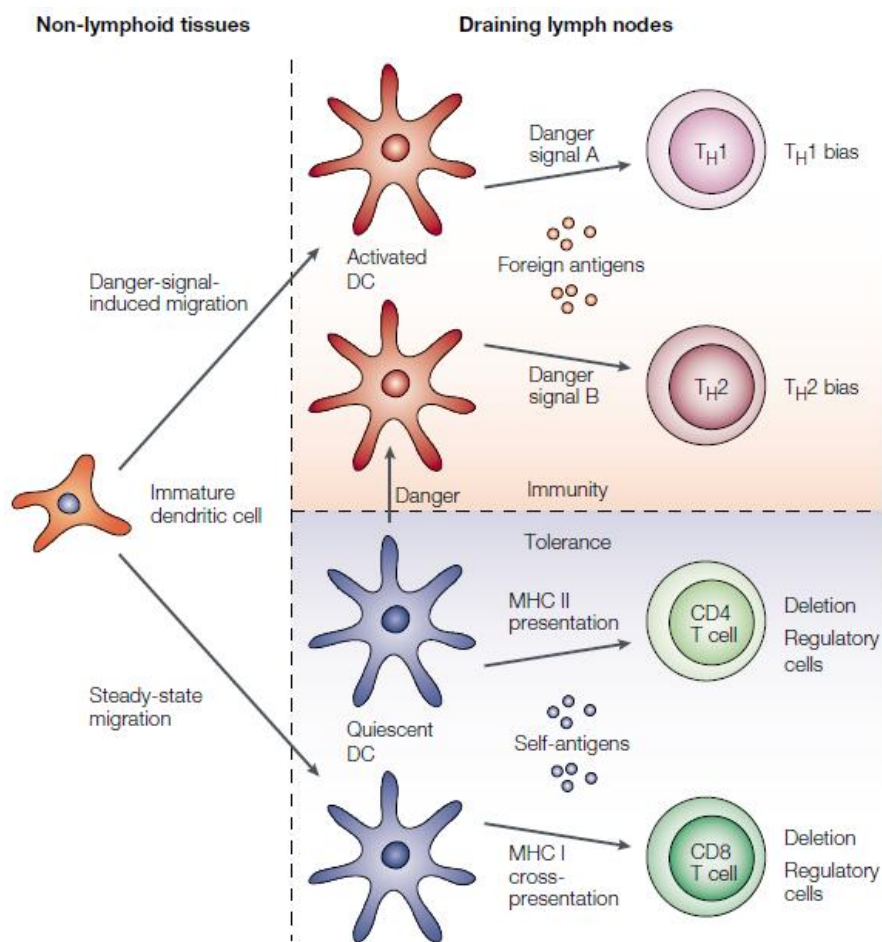


Figure 1.2. A simplified model of possible T-cell responses. The immature DC can receive a danger signal and induce T_H1 and T_H2 activation leading to an immune response against foreign antigens, or it can migrate to the lymph nodes in a steady state and present self-antigens on MHC I and II to $CD8^+$ and $CD4^+$ T-cells, thus inducing tolerance. From (22).

As illustrated in figure 1.3, DCs will interact with the T-cell receptor (TCR) with either MHC I or II and an antigen. This is the first signal to activate the T-cell. The second signal is most commonly the binding of co-stimulatory B7 molecules (CD80 or CD86) to the T-cells CD28. There are several types of secondary signals, but the CD28-CD80 and CD28-CD86 interactions are the best described and considered the most powerful. During the activation, the T-cell starts expressing new molecules including CD154 (also known as CD40 ligand) that reacts with CD40 on the DC, to further upregulate CD80 and CD86. The cycle of signals by the DC will repeat and amplify until the T-cell is fully activated and starts to synthesize IL-2 that works both autocrine and paracrine to other T-cells. IL-2 promotes T-cell proliferation and further activation of immune cells, including T- and B-cells (10,11).

The result of activation differs largely depending on the T-cell type, which can be divided into CD4⁺ and CD8⁺ T-cells (10).

CD4⁺ T-cells make up the majority of T-cells in the body, and there are several subtypes. T-helper cells (T_h) recognize antigens presented in complex with MHC II on the APC. T_h-cells are further divided into T_h1, T_h2 and T_h17 with T_h1 being specialized in the production of IFN- γ , IL-2 and TNF- β , to help induce and maintain cytotoxicity along with being known to induce delayed type hypersensitivity. T_h2 is known for the secretion of IL-4, IL-5, IL-9, IL-10 and IL-13, cytokines that establishes a strong antibody response. Some of the T_h2 cytokines (e.g. IL-10) is known to suppress T_h1-cells, and T_h1 cytokines are inhibitory to the humoral immune responses that T_h2-cells initiate. The T_h1 and T_h2-cell types are therefore inhibitory to each other, and if either the T_h1 or T_h2 is dominant, a positive feedback mechanism will maintain the dominant T_h response. Although T_h1 and T_h2 are the 2 major subtypes, other T_h-cells exist. T_h0 is a mix between T_h1 and T_h2 that produces both IL-4 and IFN- γ , but will shift towards a T_h1 or T_h2 subtype depending on the dominant response. T_h17 is a more recently discovered T_h subtype, unique in its production of IL-17 and their anti-microbial properties in mucosal barriers, and pathologically playing a major role in some autoimmune diseases (e.g. multiple sclerosis) (10,18,19).

Another type of CD4⁺ T-cell is the regulatory T-cell (T_{reg}) which has functions opposite to the T_h-cells. T_{reg}-cells suppress T_h and other immune cells activity (e.g. some B cells, granulocytes and other cell types) and maintain self-tolerance. It is believed that T_{reg}-cells play a major role in the prevention of autoimmune diseases and suppression of allergy and asthma. T_{reg}-cells are activated much like the T_h-cells (as described previously), but have a very specific affinity for the interaction with MHC II – if the signal is too weak, it will become a regular T_h-cell, but if the signal is too strong, and the cell will undergo apoptosis. Therefore, when a T-cell population is activated, a mix of T_h and T_{reg} cells will be generated, and the T_{reg}-cells will maintain

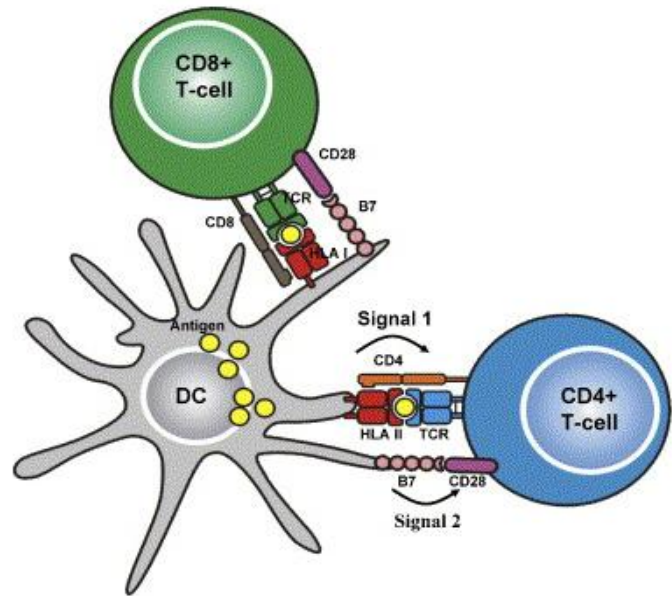


Figure 1.3. CD8⁺ T-cell and CD4⁺ T-cell activation. CD8⁺ T-cells binds to MHC I and an antigen peptide with TCR, CD4⁺ T-cells binds to MHC II along with either CD8 or CD4 for the first activation signal. B7 (CD80 and CD86) molecules on the DC binds to CD28 on the T-cells for the second signal. From (67).

self-tolerance by inhibiting the T_H-cells response to self-antigens (10,20,21).

CD8⁺ T-cells are called cytotoxic T-cells (T_C) and recognize antigens on MHC I. The activated T_C-cell is dependent on cytokines from T_H-cells to differentiate into a cytotoxic functionality, i.e. IL-2, IL-4, IL-6 and IFN- γ . The T_C-cell is able to produce all of these cytokines, although in levels too low to induce autocrine differentiation. The T_C-cell has several cytotoxic mechanisms for the killing of cells and microorganisms expressing the antigens presented to it by the APC; perforin, proteases, TNF- α and - β and nitrogen oxide. The T_C-cells are therefore often described as the soldiers of the immune system, as they are the effector cells that “search and destroy” any cell and organism expressing the foreign antigen (10).

1.1.4 Dendritic cell subpopulations

DCs are divided into different subtypes distinguished by phenotype, localization and function. Human DCs lack both specific and lineage (lin) markers (e.g. CD3, CD14, CD19, CD56) and therefore a panel of markers has to be used to identify DCs and their separate subtypes. Although the different subpopulations of DCs share many characteristics, it is unlikely that they originate from a unified DC lineage, but rather enters different differentiation paths. It is believed that conventional DCs (cDC, also known as classical DCs) originate from the common myeloid progenitor and plasmacytoid DCs (pDC) originate from the common lymphoid progenitor which both originate from the hematopoietic stem cell in the bone marrow (22,23).

1.1.4.1 Conventional dendritic cells

cDCs are the “original” dendritic cells discovered by Steinman and Cohn in 1973. The term cDC refers to any DC that is not a pDC (23), and these cells are distinguished by location and expression profile; an overview can be found in figure 1.4.

cDCs in the blood and lymphoid tissues

Two main subsets of cDCs are found circulating the blood; CD1c⁺ (BDCA1) and CD141⁺ (BDCA3) DCs. CD1c⁺ DCs makes up the most predominant subset in the blood. Cells from this subset is able to produce high amounts of interleukin 12 (IL-12) and cross-present antigens to CD8⁺ T-cells – although not nearly as effectively as the CD141⁺ subset (23).

CD141⁺ represents a minority of blood circulating DCs that uniquely express CLEC9A, are major producers of interferon beta (IFN- β) and very effectively cross-present antigens to CD8⁺ T-cells (23,24).

CD11c is expressed by all cDC subtypes, but also on macrophages and monocytes, which complicates the use of CD11c as a lineage marker for DCs in human models (23).

cDCs in the skin

Langerhans cells (LCs) is a very unique type of DC localized in the epidermis, replenished by precursors residing in the same area. LCs are completely independent of precursors circulating in the blood, and therefore adapted as a DC very differently from those in the blood and lymphoid tissues (25). LCs can be distinguished by their high expression of Langerin (CD207) and CD1a (23,26).

At least two defined subsets of cDCs have been found in the dermis layer of the skin, CD1a⁺CD14⁻ and CD1a⁻

CD14⁺ DCs. Dermal CD1a⁺CD14⁻ cells are very close to LCs in function and phenotype, CD1a⁻CD14⁺ DCs are able to induce differentiation of CD4⁺ T-cells that can induce B-cells to switch isotype and differentiate into IgG-secreting cells (27).

Recently, a third dermal DC subset was identified with CD141⁺, but not much is known yet other than its unique ability as a dermal DC to express TLR3 and CLEC9A much like the blood circulating CD141⁺ DC (23,28).







	pDC	cDC CD1c ⁺	cDC CD141 ⁺	LC	cDC CD14 ⁺	cDC CD1a ⁺
						
Phenotype:	Lin ⁻ HLA-DR ⁺ CD11c ^{low} CD1a ⁻ CD123 ^{hi} CD303 ⁺ CD304 ⁺	Lin ⁻ HLA-DR ⁺ CD11c ⁺ CD1a ⁻ CD1c ⁺ CD141 ^{+/-} CD11b ^{low}	Lin ⁻ HLA-DR ⁺ CD11c ⁺ CD1a ⁻ CD1c ⁻ CD11b ^{low} CD141 ⁺ Necl2 ⁺ Xcr1 ⁺ Clec9a ⁺ Dec205 ^{hi}	Lin ⁻ HLA-DR ⁺ CD11c ⁺ CD1a ⁺ CD14 ⁻ CD1c ⁺ Langerin ⁺ EpCAM ⁺ Sirpα ⁺ CD11b ^{+/-} E-cadherin ⁺	Lin ⁻ HLA-DR ⁺ CD11c ⁺ CD1a ⁻ CD14 ⁺ CD1c ⁺ Langerin ⁻ EpCAM ⁻ DC-SIGN ⁺ FXIIIa ⁻ CD163 ⁻	Lin ⁻ HLA-DR ⁺ CD11c ⁺ CD1a ⁺ CD14 ⁻ BDCA1 ⁺ Langerin ⁻ EpCAM ⁻ Sirpα ⁺ CD11b ^{hi}
PRRs:	TLR1 ⁺ , TLR2 ⁻ , TLR3 ⁻ , TLR4 ⁻ , TLR6 ⁺ , TLR7 ⁺ , TLR8 ⁻ , TLR9 ⁺	ND	TLR1 ⁺ , TLR2 ⁺ , TLR3 ⁺ , TLR4 ⁻ , TLR6 ⁺ , TLR7 ⁻ , TLR8 ⁺ , TLR9 ⁻	TLR1 ⁺ , TLR2 ⁺ , TLR3 ^{lo} , TLR4 ⁻ , TLR6 ⁺ , TLR7 ⁻ , TLR8 ⁻ , TLR9 ⁻	ND	ND
Murine equivalent:	pDC	cDC	CD8 ⁺ cDC	LC	ND	Dermal cDC
Location:	Blood and lymphoid tissue			Cutaneous tissue		
				Epidermis	Dermis	

Figure 1.4. Different human DC subtypes. The phenotype and PRRs for each of the established 6 DC subtypes in human is listed along with the putative murine equivalents and location of the subtype. CD1c (BDCA1), CD303 (BDCA2), CD141 (BDCA3), CD304 (BDCA4), LC (Langerhans cell), ND (not determined). Modified from (23).

1.1.4.2 Plasmacytoid dendritic cells

The pDC subtype was first discovered in the early 1990's by Alm, Fitzgerald-Bocarsly and Trinchieri. They characterized them as a subset of leukocytes producing high levels of IFN. Another independent group characterized a precursor of the pDC; they called it a plasmacytoid monocyte that could be used to generate DCs *in vitro*. Initially, the newly discovered DC subtype was named DC2, and it wasn't until the very late 1990's that it was given the name pDC. Their morphology is a lot like plasma cells and lacks the characteristic dendrites and veils that cDCs typically display (29).

pDCs are rare in peripheral blood (0.3-0.5 %) (29), and are characterized by a CD45⁺, CD11c⁺ and MHC II⁺ phenotype like cDCs – although immature pDCs express rather low levels of MHC II and CD11c compared to cDCs. CD303 (BDCA2) and CD304 (BDCA4) are specific markers for the pDCs. An overview of the expression profile for pDCs can be found in figure 1.4. Additionally, they express lower levels of the co-stimulatory molecules CD80 and CD86 in the immature state. MHC II and the co-stimulatory molecules are upregulated following the encounter with an antigen and activation, although not quite as efficient as the cDC (23). The pDCs are involved in several immunological responses; allergy and asthma, anti-tumor immunity and responses to pathogens. Their high production of IFN- α and - β makes them very important in anti-viral immune responses as well (29).

1.1.4.3 Monocyte-derived dendritic cells

The most commonly used human DCs for experiments are the monocyte-derived DCs (moDC) which are generated from CD14⁺ monocytes by culturing them with GM-CSF and IL-4 as an *in vitro* model for cDCs. It was hypothesized that moDCs represents an inflammatory boosted cell type and not identical to the *in vivo* circulating blood cDCs. Blood circulating DCs express CD123 and lack CD209, opposite to moDCs that does not express CD123 but CD209 in low levels. The expression of MHC II, CD40 and CD86 has been shown to be approximately the same on both DC types. CD83 is readily detected on DCs but not on immature moDCs, and only in low amounts on matured moDCs. Morphology differs slightly between moDCs and circulating DCs – moDCs are larger cells with irregular cytoplasm and much more prominent dendrites than circulating DCs when matured (30).

Furthermore, circulating DCs have been shown to be more effective in the activation of T-cells and induce 5-8 fold more T-cell proliferation than moDCs (30).

1.1.5 DC surface markers

This section highlights some of the most common surface markers used to identify the human DC and its subtypes.

Major histocompatibility complex I and II

MHC I is expressed on nearly all cells in the body, and is a part of the endogenous pathway of presenting antigens to CD8⁺ T-cells. MHC II is only present on APCs and is part of the exogenous pathway of presenting antigens to CD4⁺ T-cells to trigger an immune response. Surface MHC II molecules have a very short half-life in immature DCs and are continuously internalized. When the DC matures, a rapid synthesis of MHC II begins and the molecules are no longer internalized, but expressed on the surface with greater stability (11,31). MHC loading of antigens was described in section 1.1.1.

Co-stimulatory molecules; CD80, CD86 and CD40

The B7 family of co-stimulatory molecules consists of CD80 (B7.1) and CD86 (B7.2). Both markers are expressed by APCs and acts as ligands for CD28, thereby contributing to the activation of T-cells. CD40 is upregulated on the DC after phagocytosis and following maturation, enhancing antigen presentation and activation of T-cells by binding to CD154 (CD40L). CD80, CD86 and CD40 are often used for flow cytometric analyses to quantitatively determine DC maturation as they are all expressed in very low levels in the immature state and significantly higher in the mature state (10,13,32-34).

CD83

CD83 belongs to the immunoglobulin superfamily of receptors, and is expressed mainly on DCs, but can also be found on T- and B-cells. It is believed that CD83 is involved in regulation of antigen presentation by DCs, and the soluble form of CD83 has been found to inhibit DC maturation (35,36).

CD1 family

The CD1 family (CD1a, CD1b, CD1c, CD1d, CD1e) of transmembrane glycoproteins are structurally very similar to MHC molecules, and are specialized in the presentation of lipid and glycolipid antigens to T-cells (37). A study has shown that CD1a, CD1b, CD1c and CD1d are expressed on all myeloid DCs (38), but newer studies suggest that CD1a is only expressed on LCs and CD1a⁺ dermal DCs, and CD1c only on one subset of circulating blood cDCs (23).

CD141

CD141 (also known as BDCA3 or thrombomodulin) is specific for one of the blood circulating cDC subtypes and possibly a similar dermal cDC as well (23,28). CD141 is an endothelial specific type I membrane receptor that binds thrombin, and plays a part in the regulation of clotting factors and reducing blood coagulation (39). The function of CD141 on the DC subset has yet to be discovered (28).

CD303 and CD304

CD303 (also known as BDCA2 or CLEC4C) and CD304 (also known as BDCA4 or neuropilin 1) can be used to distinguish pDCs from cDCs. CD303 is a member of the C-type lectin superfamily and is thought to play a role in IFN production in pDCs (40,41). CD304 is a transmembrane C-lectin that affects cell survival, migration and attraction and binds both vascular endothelial growth factor (VEGF) and semaphorin (42,43). It is expressed on B-cells, plasma cells and red blood cell precursors as well as pDCs (43,44).

CD11c

CD11c (also known as alpha X) is a 145-150 kD alpha chain of an integrin primarily expressed on most DCs, monocytes, and to a lower extent on tissue macrophages, NK cells, neutrophils and some subsets of T- and B-cells. It is non-covalently associated with CD18 to form a complex (alpha X beta 2 or CR4) which plays a role in cell adhesion (45-47). The complex binds to a diversity of ligands such as cell adhesion molecules (e.g. ICAMs), bacterial cell wall components (e.g. LPS), complement proteins (e.g. iC3b) and matrix proteins (e.g. collagen and fibrinogen) (47).

CD11c contains an I-domain that has been shown to be the binding site for different ligands (47-49). The I-domain consists of seven helices surrounding a β -sheet core and a metal-ion-dependent adhesion site (MIDAS). It has been proposed from structural studies that the I-domain regulates binding of ligands by being in either open or closed formation (50). The 3D structure of the I-domain for CD11c is illustrated in figure 1.5.

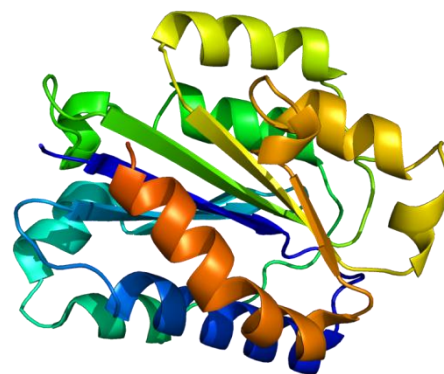


Figure 1.5. 3D structure of the CD11c molecules I-domain. From (68).

1.1.6 Human versus murine dendritic cells

To translate results from a murine DC-targeting experiment to the human system, the interspecies differences has to be known and considered to decide which targets to use and if the responses will be somewhat similar. Since murine lymphoid tissues are more readily available, more studies and extensive research has been done on the DCs in the murine system both *in vitro* and *in vivo* compared to the human system, and therefore the differences we know today may only be a fraction of what there is to be discovered. Another problem with comparing murine and human DCs is the fact that DCs are usually generated from peripheral blood monocytes in human model experiments, and DCs directly isolated from lymphoid tissues without differentiation steps is not common practice for the investigation of human DCs (22). The directly isolated mouse DCs are likely in their most natural form, whereas the human DCs have been manipulated into their form and may differ largely from natural *in vivo* differentiated DCs. It is possible to obtain moDCs from mice, but it is rarely done as isolating from lymphoid tissues gives higher DC yields than generating moDCs (51). Therefore, it is difficult to directly compare DCs from the mouse and human systems as they are rarely isolated in the same way.

One of the murine DC subtypes express CD8, although in an $\alpha\alpha$ -homodimer form rather than the $\alpha\beta$ -heterodimer that is seen in T-cells. CD8 is not expressed by any of the human DC subtypes, and it has been assumed that the CD8⁺ subset was unique for the murine system (22). However, recent studies proposed that human CD141⁺ DCs could possibly be the equivalent of the mouse CD8⁺ DCs due to the fact that they both express CLEC9A, basic leucine zipper transcription factor ATF-like 3 (plays a role in DC development), and IRF8 and lack IRF4 (IFN regulatory factors, plays a role in differentiation) (23).

CD11c is a more specific marker for DCs in the murine system than in the human system, as CD11c is also expressed on other cells in the human system as described in section 1.1.5 (23,24).

1.2 Dendritic cell vaccines

Since the first *ex vivo* DC trial in 1996 (52) we have come a long way and acquire more and more information about DCs and ways of utilizing them for vaccines every single day. Searching for the term “Dendritic cell vaccine” in the database Clinicaltrials.gov (53) yields 344 clinical studies of which more than 70 studies are currently open and recruiting. Most studies are focusing on cancer treatment, while others are exploring the options of treating HIV and malaria with DC based vaccines as well (53,54).

There are 4 approaches to DC vaccines; “random DC targeting”, *ex vivo* generated cytokine-driven DCs, targeting specific DC subsets *in vivo* and personalized therapeutic vaccines. Random DC targeting is based on antigens, viral vectors or transduced tumor cells administered with or without adjuvants to elicit an immune response. This method is non-targeted, and might therefore lead to an unwanted immune response if taken up by the wrong immune cells and there is generally very little control over the DC subset targeted. The Provenge vaccine is an example of the *ex vivo* generated cytokine-driven DCs (described in section 1), where DCs are stimulated with an antigen *ex vivo* and administered back to the patient for an immune response against the antigen. This method has a lot more control over the DCs targeted, but it is important to question the state of the DCs – as they have been stimulated *ex vivo* in an environment far from the complexity of the natural tissues and cytokine levels *in vivo*, how close they are to natural DCs, and are they as functional as DCs in their natural environment? It is believed that the effectiveness of culturing DCs *ex vivo* and injecting them back into the patient is rather low, and many of the DCs never make it to lymph nodes to activate T-cells. Therefore, more research is now focused on targeting specific DC subsets *in vivo* by fusing an anti-DC antibody (e.g. CD205, CD40, CD11c, Langerin) with an antigen and most often a DC activation adjuvant as well (e.g. Poly I:C). This method is thought to solve some of the problems with *ex vivo* generated DCs as this approach exploits the DCs present *in vivo*. Another problem that could be solved with this method, is the problem of targeting specific cells – by choosing an appropriate antibody, it may be possible to target specific subsets of DCs. Personalized therapeutic vaccines are the next step in the history of DC vaccines; this method is focused on adjusting vaccines to individual patients. The method is much like the targeting of DCs *in vivo*, but with added adjuvants to help break down the suppressiveness of the tumor micro-environment by for example inhibiting Treg cells or the silencing suppressor of cytokine signaling 1 (SOCS1) to increase immunogenicity against weakly immunogenic tumors. The “cocktail” of antigens, antibodies and adjuvants is personalized for the patient, depending on the type of cancer. The last method is a fairly new field of personalized vaccines that more and more research is moving towards (11,54,55).

There are a lot of considerations one has to make before engineering a DC vaccine: 1) which DC subset to target, 2) which molecule on these to target, 3) which antigens and adjuvants to use, 4) which T-cells should be activated, 5) will the T-cells know where to migrate to, and 6) is the aim prevention of disease or therapeutic treatment.

The importance of choosing the right DC receptor to target is crucial – it decides if you will be targeting a single DC subset or the whole DC population or maybe even other cells than DCs. And the question is; what happens if cells other than DCs take up the vaccine? (11,54).

Some tumors have been found to not express their own unique antigens, in which case it would be very difficult to create a vaccine against these types of tumors. The ones that do however, are theoretically the easier ones to target and eventually treat with a DC vaccine. If the vaccine is administered in the absence of

adjuvants, it could potentially lead to tolerance – this could however, be exploited in the treatment of autoimmune diseases. Adjuvants are vital in DC vaccines as they help with the activation and maturation of DCs so that they don't end up inducing a tolerance to the antigens received in a vaccine.

Polyinosinic:polycytidylic acid (Poly I:C) is a commonly used adjuvant in vaccines that acts as a TLR3 agonist that activated DCs. Other adjuvants can be chosen to help the vaccine – for example, Suppressor of cytokine signaling 1 (SOCS1) works as an attenuator of the antigen presentation process in DCs, and by inhibiting SOCS1, the immunogenicity to the antigen is enhanced (54-56).

Another crucial point is which T-cells will be activated and how to make sure they migrate to the tumor site. Both CD4⁺ and CD8⁺ T-cell activation has been shown possible in mouse models (6), but to activate CD8⁺ T-cells, the vaccine must be able to let the antigens be presented on MHC I molecules for cross-presentation. The vaccine must be internalized efficiently, processed and then presented on both MHC I and II for optimal T-cell responses. For example, CD40 has been shown to have poor internalization properties but was very efficient at cross-presenting antigens directed to the receptor, whereas CD205 was better at internalizing and had very poor cross-presenting functionality (57). Therefore, for a better CD8⁺ T-cell response CD40 would probably be chosen as the target receptor, since CD205 would most likely not elicit a very strong CD8⁺ T-cell response. CD11c looked promising as a cross-presenting target as well.

Lastly, is the vaccine meant to work as preventative treatment or therapeutic treatment? Cellular activation is very important for a therapeutic vaccine to treat and eliminate the current tumor, where humoral activation would be better for a preventative vaccine since long-lived memory B-cells with information about cancerous antigens could help keep the body immune to certain types of cancers when the antigens are expressed on the surface of the cancer cells (54,55).

1.3 CD11c – a candidate target for future targeted vaccines

Some research on the use of CD11c as a target for DC vaccines in the murine system has been done, and some of the most significant studies and findings from the murine model are outlined below.

Castro *et al.* investigated the use of ovalbumin (OVA) conjugated to a Fab' fragment specific for CD11c, CD40, CD205 and MHC II. The conjugates were added to bone marrow derived DCs (BMDC) and proliferation of T-cell types OT-I (CD8⁺) and OT-II (CD4⁺) was analyzed 72 hours later. The T-cell proliferation from DCs cultured with the CD11c conjugate was relatively low compared with CD40, CD205 and MHC II. The group then repeated the experiment, but used a splenocyte culture instead of BMDCs as APCs with the rationale that this would be closer to what would be observed *in vivo*. In this experiment, T-cell proliferation responses were much higher for CD11c for both OT-I and OT-II compared to the other targets (6).

Castro *et al.* proceeded to perform *in vivo* experiments, in which mice were immunized with the OVA-conjugated Fab' fragments specific for CD11c, CD40, CD205 and MHC II, as well as agonistic anti-CD40 (to promote immunization) and administered CFSE-labeled OT-I and OT-II T-cells 1, 4 and 7 days later. Results showed that both OT-I and OT-II T-cell proliferation was very high for the CD11c conjugate, higher than for CD40, CD205 and MHC II. Subsequently, they investigated the ability of the activated CD8⁺ T-cells to be effector cells and kill target cells by injecting OVA pulsed cells i.p. They observed that the T-cells activated by APCs stimulated with the CD11c-OVA conjugate had a 90% killing of target cells compared to 50-60% for

CD205 and even lower for MHC II. Additionally, they investigated the accumulation of the conjugates and it turned out that the CD11c fragment accumulated with almost 100% in the spleen, and none in the lymph nodes (6).

They concluded that CD11c may be an unusually effective target for future vaccines from the results in both *in vitro* and *in vivo* experiments (6).

Cruz *et al.* used a nanoparticle carrying OVA, Poly I:C (TLR3 agonist) and TLR7 ligand R848 (a imidazoquinoline compound that activates immune cells through TLR signaling), and conjugated it with antibodies against CD11c, CD40 or CD205. They investigated binding and internalization of the nanoparticle, and concluded that all targets were bound and internalized with significant differences compared to the non-targeted control *in vitro*. Furthermore, they analyzed the activation and maturation of BMDCs after binding of the nanoparticle with flow cytometry using the maturation markers CD40 and CD86. They found that more than 90% of the BMDC population matured after being cultured with the 3 differently targeted nanoparticles after 24 hours. Lastly, before moving on to *in vivo* studies, they investigated the T-cell activation by culturing the DCs treated with the nanoparticles in co-cultures with splenocytes from OT-I and OT-II mice. The results showed significant increases in proliferation of the OT-cells for all targets compared to the non-targeted controls. Cruz *et al.* then moved on to *in vivo* experiments, where C57BL/6 mice were vaccinated with the nanoparticles (described earlier) and 7 days later given CFSE labeled OVA-expressing target cells. Cytotoxicity was then assessed with flow cytometry 18 hours later to determine the killing of the target cells, and results showed an 80% specific killing for the different targeted nanoparticles compared to 40% non-specific killing in controls. CD11c performed well in all experiments by Cruz *et al.*, but did not seem to be a better target compared to CD205 and CD40 (5).

Ejaz *et al.* investigated the possibility of vaccinating mice against viral infections by targeting DCs with CD11c-specific single chain variable fragments (scFv) fused to an immunodominant peptide of Friend retrovirus. They co-cultured Friend virus specific T-cells with BMDCs that were cultured with the vaccine construct and demonstrated that T-cell activation was significantly higher compared to the controls. The group conducted an *in vivo* vaccine challenge using C57BL/6 mice which were vaccinated with BMDCs loaded with the CD11c-targeted peptides twice in one-week intervals. The animals were then challenged with Friend virus one week after the last vaccination and results showed that significantly fewer mice were infected with the virus 4 days post infection compared to the controls (2).

Wei *et al.* fused a CD11c-specific scFv to human epidermal growth factor receptor 2 (HER2/neu), mixed it with DC-activating CpG (an oligodeoxynucleotide consisting of cytosine and guanine linked by a phosphodiester bond) and vaccinated BALB/c and BALB/neuT mice (expressing a transforming neu under the control of mouse mammary tumor virus promoter) with the peptide on day 0 and 7. On day 14, the mice were inoculated with D2F2/E2, D2F2 or TUBO tumor cells expressing HER2 and tumors size was measured. All vaccinated animals were tumor free compared to the control animals which all had an almost exponential increase in tumor volume over 60 days. A rechallenge approximately 3 months after the first vaccination showed that the vaccine was still effective as newly inoculated D2F2/E2 tumor cells did not proliferate. To determine if the vaccine could be used therapeutically in addition to protectively, BALB/c mice were injected with D2F2/E2 tumor cells and given the vaccine on day 8 and 15. The treatment substantially slowed tumor growth, and protected up to 80% of the mice from tumor growth where the controls had no inhibiting effect on the growth of tumors (7).

Results from the 4 studies all suggest that CD11c is a very effective target for a DC vaccine in murine models, however, very little information about internalization of anti-CD11c alone is available. Even less information can be found about the features of human anti-CD11c and how it interacts with human DCs. One of the reasons CD11c is as effective a target for antigens in mice, is possibly the fact that some CD11c antibodies induce maturation in DCs (5). It would be interesting to discover if the same interaction with CD11c in the human system would lead to DC maturation as well.

Since CD11c is not expressed only on DCs in the human system, it would be interesting to see what other cells express the molecule. There is no general consensus about the distribution of CD11c in the human system, but most agree that CD11c is found on monocytes, and to some extent macrophages as well (23). Some believe that CD11c is also expressed on NK cells and neutrophil granulocytes as well (47).

To take the step further and investigate how effective CD11c would be as a target for human DC vaccines, it is crucial to know how CD11c is distributed in tissues in order to know what other cells might be affected by anti-CD11c other than DCs.

1.4 Flow cytometry

Flow cytometry is a commonly used method in immunology that makes it possible to count and examine a cell population by size and/or surface markers. Cells are stained with fluorochrome-conjugated antibodies against the cell surface molecules of interest prior to the analysis and suspended in azide or formaldehyde. Flow cytometry measures the optical (size and granulation) and fluorescence (intensity) of each cell analyzed (58). A simplified model of flow cytometry is illustrated in figure 1.6.

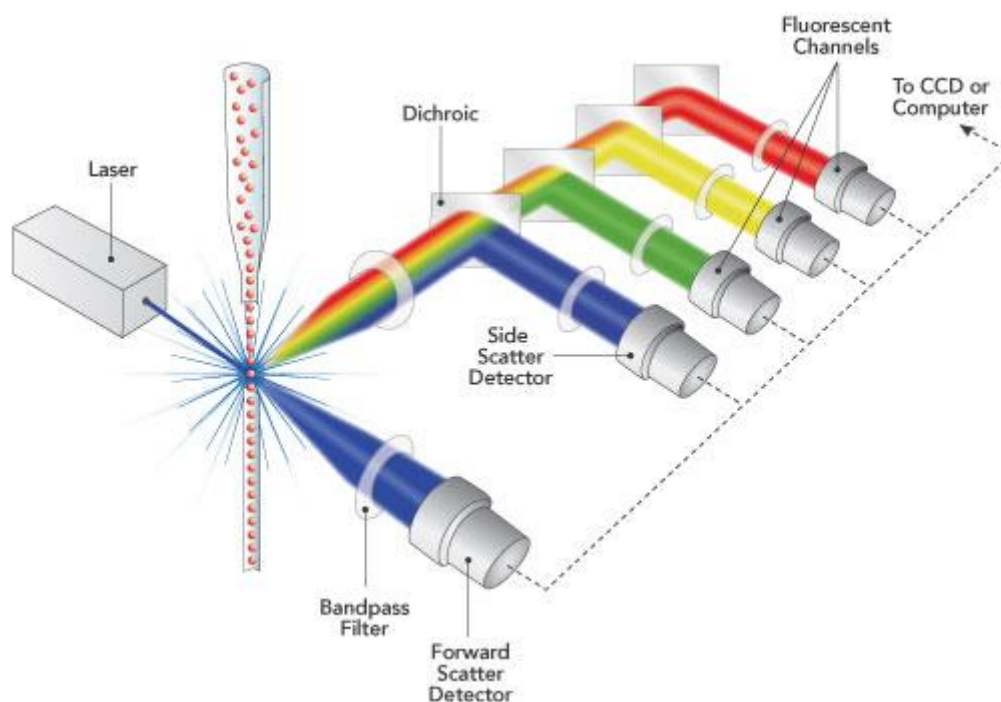


Figure 1.6. A simplified model of the optics part of the flow cytometer. The figure shows a setup with one laser and measurement of three colors of fluorescence. A laser beam is directed to the single cells and emission hereof is directed to different detectors through filters and dichroic mirrors. From (58).

The cell suspension is drawn into a stream of sheath fluid in the flow cytometer, and single cells (also called events in flow cytometry) pass by a point where beams of monochromatic light from a laser hit. This results in emitted light from the cells and the fluorochromes bound to them, and the emission is collected by optics that direct the light to different filters and dichroic mirrors. The dichroic mirrors isolate certain wavelengths of the light – as seen in figure 1.6, 3 different wavelengths of light is isolated by dichroic mirrors. The isolated light is directed into their respective detectors and measures the fluorescence of the cell. 2 other detectors collect light scattered by forward and side angles; forward scatter measures the spread of the light waves and is a direct measure of the size of the cell, whereas side scatter measures the intracellular granulation. The data of the collected light is then converted to digital numbers to the computer and visualized in scatter plots and histograms (59).

It has become standard practice to use isotypes for each sample analyzed. The reason for this is to rule out any non-specific Fc receptor binding that can create false-positive events. This is especially important when working with cells with many Fc receptors, such as dendritic cells and monocytes. The isotype needs to match the primary antibody; it has to be from the same host species, from the same immunoglobulin class

and be conjugated to the same fluorochrome as the primary antibody (60). When working with multicolor samples, it is very important to obtain accurate data by creating a compensation matrix prior to the analysis to correct for any possible spillover between the fluorochromes used. Spillover occurs when the emission spectra of fluorochromes overlap, an overview of 4 fluorochromes used in this project is illustrated in figure 1.7.

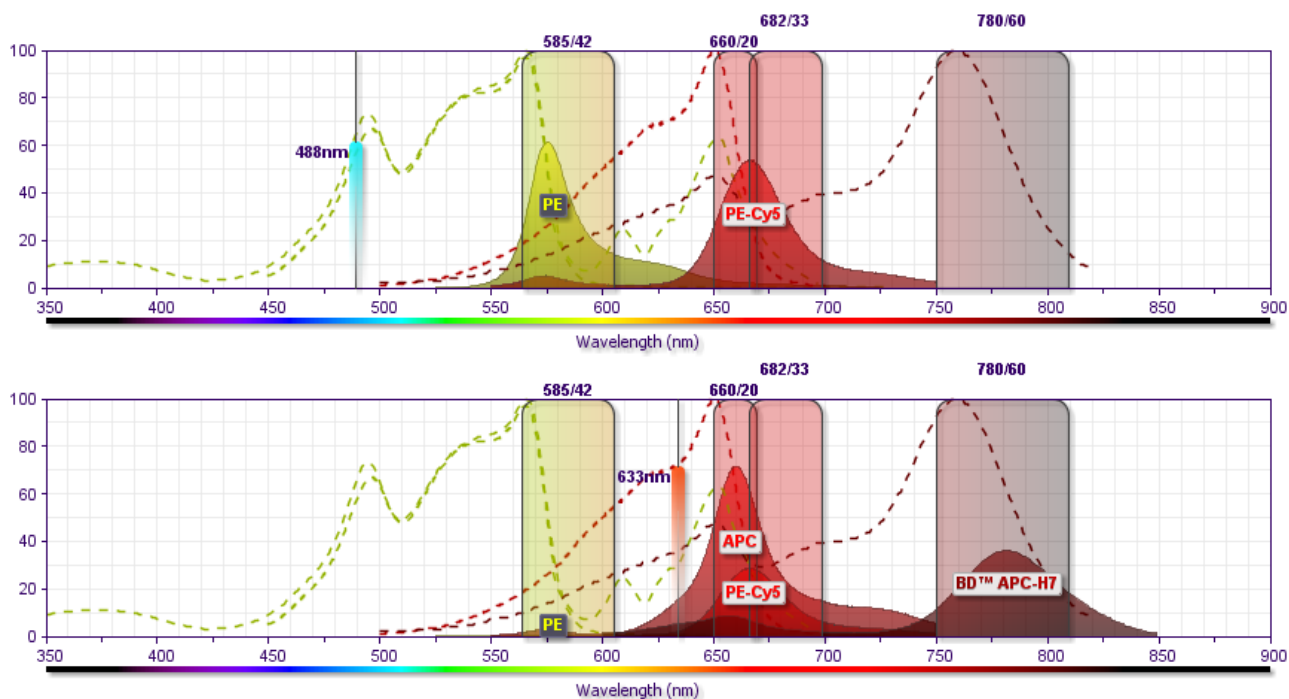


Figure 1.7. Fluorochrome spillover with 4 fluorochromes and 2 lasers. Blue laser (488 nm) excites PE and PE-Cy5 fluorochromes, with minimal spillover. Red laser (633 nm) excites PE-Cy5, APC and APC-H7 with very much spillover from APC into PE-Cy5 and some from PE-Cy5 into APC-H7. X-axis represents a normalized fluorescence intensity and the Y-axis represents the wavelength. Generated from (69).

A compensation matrix is created by measuring the fluorochromes individually to determine their exact spectra of emission and then analyze their overlap. The spillover values are placed in a matrix, in which it is possible to calculate the compensation values to correct for any spillover in other detectors than what is desired. It is possible to calculate the compensation values by hand with matrix algebra, but this is a tedious task and flow cytometry analysis programs can do it in seconds. A computer generated compensation matrix that was used for analyses for this project is illustrated in figure 1.8.

Spillover (%)				
	PE	Pe-Cy5	APC	APC-H7
PE		2,03	0,51	0,00
Pe-Cy5	9,69		0,41	0,11
APC	0,31	82,34		2,12
APC-H7	0,09	11,68	8,04	

Figure 1.8. Compensation matrix with 4 fluorochromes. Spillover was calculated for individual fluorochrome samples and the matrix was generated by FACSDiva (Beckton Dickinson) and is here displayed by the Kaluza analysis program.

1.5 Confocal microscopy

Confocal microscopy is used to visually analyze cells that were stained with fluorochromes, and is much more precise than ordinary fluorescence microscopy in the way that it is more specialized in controlling the depth of field and filtering out background information from nearby layers, thereby providing a much more high quality image than what can be obtained in a regular microscope. A simplified model of a confocal microscope and the laser beams path is illustrated in figure 1.9. Light is emitted from a laser excitation source (many microscopes has several lasers) and passes through a light source pinhole aperture and excitation filter. The laser beam is then directed to the specimen by being reflected by a dichromatic mirror and passed through the objective. As the laser beam reaches the point in a defined focal plane, the fluorescence emitted from the specimen passes back through the objective and dichromatic mirror, and reaches the detector pinhole aperture. From here, the focused light is sent to a photomultiplier detector that sends information about the image to the associated computer. Any light rays that are out of focus do not go through the detector pinhole aperture, and therefore will not reach the photomultiplier detector.

The many apertures allow the operator to control the thickness of the focal plane section, which highlights one of the main differences between widefield and confocal microscopes. Widefield microscopes focuses on a wide cone of illumination of the specimen, but confocal microscopes focus on a much narrower focal plane and filter out any illumination of the rest of the specimen below and above the focus plane.

To capture an image with the confocal microscope, 2 mirrors moves along the X- and Y-axis of the specimen to move the focused laser beam and the end result is an image generated from “scan lines”. The more scan lines is chosen, the more high resolution the image will be but also takes longer to capture, which is important to consider if using fluorochromes that are very photo sensitive (61).

It is important to include controls; an unstained control to determine the level of autofluorescence from the cells alone and secondary-stain only controls to rule out any unspecific binding of the secondary antibodies. Fixing in between staining steps helps to eliminate any cross-binding when using multiple fluorescent antibodies by stabilizing them after their binding to the cells (61).

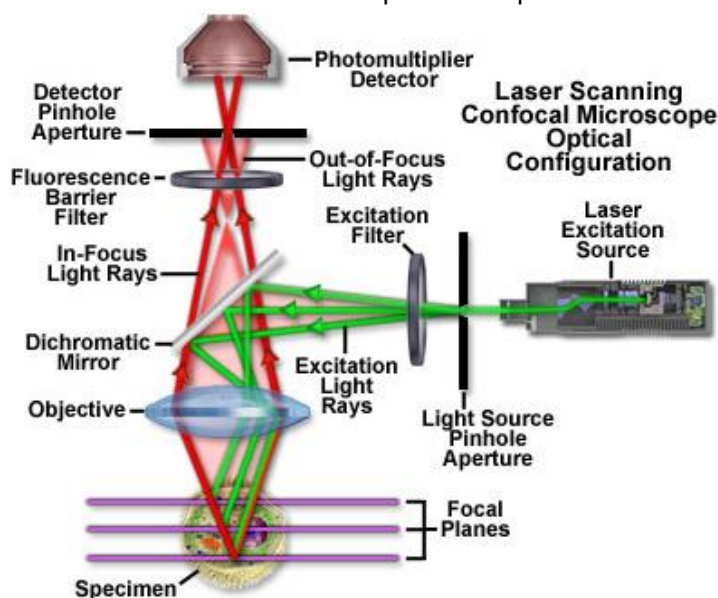


Figure 1.9. A simplified model of a confocal microscope. The laser beam is directed through filters and dichromatic mirrors through the objective to the specimen, and emitted light is directed back through more filters and apertures for a high resolution image. From (61).

2 Study aim

There are many research papers to be found with information about murine DCs and CD11c from both *ex vivo* and *in vivo* experiments, but not much is published about CD11c on human DCs. To use CD11c as a potential target for a future DC vaccine, it is therefore crucial to increase our knowledge about all properties of human CD11c and how targeting this molecule affects human DCs. The primary aim of this study is therefore to investigate how CD11c antibodies interacts with human DCs and is the first step in the process of converting a murine vaccine construct to targeting murine CD11c, into one that can be used in a human model.

Hypotheses:

1. In man, CD11c is expressed on dendritic cells and other antigen-presenting cell types
2. Exposure to antibodies against CD11c will induce maturation of developing moDCs
3. Antibodies against CD11c will be internalized by moDCs
4. Antigens internalized via CD11c will effectively become processed and presented on MHC II

3 Materials and methods

3.1 Isolation of PBMCs

Peripheral blood (50-80 ml per experiment) was collected from a healthy volunteer and diluted 1:2 with RPMI1640 (Invitrogen, 42401018) in 15 ml centrifugation tubes (VWR, 21008-216). Lymphoprep (Medinor, 1114545) was carefully injected into the bottom of the tube, under the diluted blood. Tubes were centrifuged at 180 *g* for 20 minutes at room temperature with acceleration set to 2 and break 0. Approximately 25 % of the supernatant was removed, and tubes were centrifuged again at 380 *g* for 20 minutes at room temperature with acceleration 2 and break 0. The PBMCs were harvested by carefully collecting the interphase with a Pasteur pipette (Copan, 200CS01), and pooled in new centrifuge tubes containing cold PBS (Gibco, 2012-019) + 1 mM EDTA (Sigma, E5134). The PBMCs were washed 3 times with PBS + 1 mM EDTA and pooled after each wash. The first two washing steps were centrifuged at 300 *g* for 10 minutes at 4 °C with acceleration 2 and break 0. The last washing step was centrifuged at 200 *g* for 10 minutes at 4 °C with acceleration 2 and break 2. After the last washing step, the PBMCs were resuspended in cold buffer containing PBS + 2 mM EDTA + 0.5 % BSA (Sigma, A2153) and counted in a haemocytometer.

3.2 Monocyte isolation

PBMCs were centrifuged at 300 *g* for 10 minutes at 4 °C with acceleration set to 5 and break 2. The supernatant was removed and the PBMCs were resuspended in 30 µl buffer (PBS + 0.5 % BSA + 2 mM EDTA) per 10⁷ total cells. 10 µl per 10⁷ total cells FcR Blocking Reagent and Biotin-Antibody Cocktail from the Monocyte Isolation Kit II (Miltenyi, 130-091-153) were added, and the PBMCs were incubated for 10 minutes at 4 °C. The buffer containing PBS + 2 mM EDTA + 0.5 % BSA was added along with 20 µl per 10⁷ total cells Anti-Biotin Microbeads from the Monocyte Isolation Kit II and the PBMCs were incubated for an additional 15 minutes at 4 °C. The PBMCs were then centrifuged at 300 *g* for 10 minutes at 4 °C with acceleration 5 and break 2. The supernatant was removed completely and the PBMCs were resuspended in cold buffer. The MACS system was set up and the column rinsed with buffer. The PBMCs were poured into the column with 3 subsequent rinsing steps with buffer to get all the monocytes through the column. The collected monocytes were centrifuged twice at 300 *g* for 10 minutes at 4 °C with acceleration 5 and break 2. The supernatant was removed completely after each centrifugation, and the monocytes were resuspended in RP10 medium (RPMI1640 + 2 mM L-Glutamine (Invitrogen, 21051-024) + 10 % FCS (from colleagues in the LSR group, lot. 41G2300K) + 1 % Penicillin/Streptomycin (Sigma, P433)). The monocytes were counted in a haemocytometer and set to a concentration of approximately 5 x 10⁵ cells/ml. In some pilot experiments, monocytes were isolated using CD14 microbeads (Miltenyi, 130-050-201) following the same procedure as described, with the exception of incubation times and magnetic separation. The microbead labeling only requires 15 minutes of incubation time in one step, and the isolated monocytes are positive, therefore eluted into a collection tube after magnetic separation in the column.

3.3 DC differentiation

Monocytes were isolated as described above and cells were adjusted to a concentration of 5×10^5 cells/ml. Cytokines were added prior to seeding 6 ml cell suspension in a 6 cm cell culture dishes (Nunc, 150288), GM-CSF (60 ng/ml) (Peprotech, 300-03) and IL-4 (100 ng/ml) (Peprotech, 200-04). The cell suspension incubated for 3 days at 37 °C. On the third day, 0,6 ml medium containing GM-CSF (600 ng/ml) and IL-4 (1 µg/ml) was added to the each culture dish and they were incubated for another 2 days. On the fifth day of culturing, 6 ml medium with GM-CSF (60 ng/ml) and IL-4 (100 ng/ml) was added - doubling the volume in the culture dishes to 12,6 ml. On the sixth day, a maturation stimulus in form of LPS or a CD11c antibody was added to the dishes containing DCs to be matured, followed by additional 24 hours of incubation. DCs without maturation stimulus remained immature. On the seventh day, the cells were harvested by washing with the medium in the culture dish, collecting the DCs in a centrifugation tube, and washing the culture dish with fresh medium once more to collect the remaining DCs. The collected DCs were washed, resuspended in PBS + 0.1 % BSA + 0.01 % sodium azide (Merck, 8.22335.0100) and counted in trypan blue (Sigma, 93595). The cells were now ready for immunostaining.

Prior to harvesting, pictures were taken of each culture dish with an inverted microscope (Leica DM IL) using either the 10x or the 20x objective. Pictures were taken with an external camera and edited with ImageJ (v 1.48). Pictures were taken within 2 minutes of removing the dish from the incubator, to capture an image with the DC veils and dendrites before they retracted.

3.4 Antibodies

Ultra-LEAF (low endotoxin, azide free) purified mouse anti human CD11c antibody clones 3.9 (Biolegend, 301632) and BU15 (Biolegend, 337202) were used. While both clones blocks the CD11c integrins binding to ICAM-1, 3.9 binds divalent cation dependent and only to the open formation I domain, whereas BU15 binds to CD11c in both active and inactive forms (47). LEAF purified mouse IgG1,k (Biolegend, 400165) was used as isotype control for both anti-CD11c clones.

A secondary antibody, Alexa 488 F(ab')₂ goat anti-mouse IgG (Jackson ImmunoResearch, 115-546-062) was used in a 1:50 dilution to visualize CD11c and IgG binding in the internalization assay. Mouse anti human HLA-DR-Alexa 647 (Biolegend, 307622) was used in a 1:100 dilution for the visualization of the cell membrane and internal HLA-DR compartments.

For flow cytometric analysis, the following antibodies and dilutions were used to determine DC maturity along with identifying T- and B-cells and monocytes; 1:20 HLA-DR-APC-H7 (BD Pharmingen, 561358), 1:5 CD80-PE-Cy5 (BD Pharmingen, 559370), 1:5 CD83-APC (BD Pharmingen, 551073), 1:5 CD86-PE (BD Pharmingen, 555658), 1:5 CD14-PE (BD Pharmingen, 555339), 1:5 CD14-FITC (Thermo scientific, MA1-19561), 1:5 CD3-FITC (BD Pharmingen, 555339), 1:5 CD19-APC (BD Pharmingen, 555415) and 1:20 CD11c-PE (Biolegend, 337206). Corresponding isotypes were used; 1:20 IgG2a,k-APC (BD Pharmingen, 560897), 1:5 IgG1,k-PE (BD Pharmingen, 555749), 1:5 IgG1-APC (BD Pharmingen, 555751), 1:5 IgG1,k-PE (BD Pharmingen, 555750) and 1:5 IgG1a,k-FITC (BD Pharmingen, 555573).

3.5 Flow cytometric analysis

PP tubes (Falcon, 60818-292) were labeled and prepared with antibodies according to the chart in figure 3.1. 100-500 µl of the cell suspension (minimum 100.000 cells) was added to each tube with antibodies and incubated for 30 minutes at 4 °C with tin foil covering. The cells were washed with PBS + 0.5 % BSA + 0.01 % sodium azide and centrifuged at 300 *g* for 5 minutes at 0 °C with acceleration set to 6 and break 2. Supernatant was discarded and the washing step was repeated. Cells were fixed with 1 % formaldehyde (VWR, 97131000) and ready for flow cytometric analysis. Flow cytometric analysis was performed on a BD FACSCanto flow cytometer (Becton Dickinson, 337175) with two lasers (red, excitation 633 nm, blue, excitation 488 nm). Cytometer calibration was performed before each round of analysis with BD FACS 7-Color setup beads (BD Biosciences, 335775) in the FACSCanto setup program (Beckton Dickinson, FACSCanto, V 2.1.2316). The program used for data acquisition was FACSDiva (Beckton Dickinson, FACSDiva, V 5.0.3, Firmware V 1.14). Kaluza Analysis (Beckman Coulter, V 1.3) was used for subsequent data analysis.

Multi-color tubes were analyzed with a compensation file linked. The compensation file was created prior to the experiments to compensate for any spillover. Fluorochrome charts and 4-color compensation matrix can be found in section 1.4 in figure 1.7 and 1.8.

20.000 events were recorded for cells stained with specific antibodies, 10.000 events were recorded for isotypes controls. In case there fewer cells in a sample, as many events as possible was recorded.

Few samples were run on a MoFlo Astrios flow cytometric cell sorter (Beckman Coulter, A66813).

Flow cytometric data was analyzed with Kaluza Analysis by gating the anticipated DC population and setting up overlays for each sample with antibodies and corresponding isotypes. Doublet controls was performed by plotting the sample into a forward scatter area/forward scatter height (FSC-A/FSC-H) dot plot and any occurring doublets were removed. MFI was calculated as the geometric mean of total fluorescence above 10⁰ (isotypes were below 10⁰).

Antibody	Volume in µl	Isotype	Volume in µl
HLA-DR-APC-H7 (BD, 561358)	5	IgG2a,k-APC-H7 (BD, 560897)	5
CD80-PE-Cy5 (BD, 559370)	20	IgG1,k-PE-Cy5 (BD, 555750)	20
CD86-PE (BD, 555658)	20	IgG1,k-PE (BD, 555749)	20
CD83-APC (BD, 551073)	20	IgG1,k-APC (BD, 555751)	20
CD14-PE (BD, 555398)	20	IgG1,k-PE (BD, 555748)	20
CD19-APC (BD, 555415)	20	IgG1,k-APC (BD, 555751)	20
CD3-FITC (BD, 555339)	15	IgG2a,k-FITC (BD, 555573)	15

Figure 3.1. Chart with antibodies used for cell suspensions in preparation for flow cytometric analysis.

3.6 Confocal microscopy

Rings were drawn with a PAP-pen (Sigma, 2672548-1EA) on poly-L-lysine slides (Thermo, J2800AMNZ), left to dry completely and then moved to a humid chamber. Cell suspension from the internalization assay was added to each slide (50.000-100.000 cells per slide) and after 15 minutes the supernatant was removed and replaced with 3.7 % formaldehyde. Slides were incubated at 4 °C for 20 minutes and washed. 0.2 % Triton-X (Sigma, 9002-93-1) was added to each slide, incubated for 7 minutes at room temperature and then

washed. 1:50 diluted secondary antibody Alexa 488 F(ab')₂ goat anti-mouse IgG was added to each slide and incubated for 30 minutes at 37 °C. Slides were then washed and fixed with 3.7 % formaldehyde. Slides were washed and 1:100 Alexa 647 anti-HLA-DR was added and incubated at 37 °C for 30 minutes and washed. 1:1000 DAPI was added to be able to see the cell nuclei prior to capturing images, and incubated for 10 minutes at room temperature and washed. Mounting medium (kindly provided by Svend Birkelund at the Laboratory of Medical Mass Spectrometry at Aalborg University) was added and cover slides were applied and secured with tape, and analyzed on a confocal microscope (Leica, TCS SP5 inverted) with a 100x objective and accompanying imaging software (Leica LAS AF 2.5.1.6757) according to manufacturer's instructions. Subsequent image editing was performed with LAS AF Lite (Leica v. 2.6.3) with adjustments of contrast and brightness for clearer and brighter images. Images resizing was performed in ImageJ.

3.7 CD11c distribution assay

Whole blood, PBMC, negative selected monocytes and positive selected monocytes were prepared and stained with CD11c-PE, HLA-DR-APC-H7, CD80-PE-Cy5, CD83-APC, CD86-PE, CD3-FITC, CD19-APC and CD14-PE to determine the location of populations in the analyses with the FACSCanto flow cytometer. PBMCs were prepared and stained with CD11c-PE, HLA-DR-APC-H7, CD14-FITC to determine the location of populations in the analyses with the MoFlo Astrios flow cytometric cell sorter.

3.8 Maturation assay

24 hours before harvesting, CD11c antibodies (3.9 and BU15) were added to the dishes in concentrations 1 µg/ml and 5 µg/ml. LPS (10 ng/ml) was added to a separate dish as a positive control (mature), and nothing was added to the negative control dish (immature). Cells were analyzed by flow cytometry as described in section 3.5 to determine maturation.

3.9 Internalization assay

Cells were counted and split in 3 PP tubes labeled "CD11c 3.9", "CD11c BU15" and "IgG". Antibodies were added to the tubes, and incubated on ice for 30 minutes. The cells were washed in buffer 1 (PBS + 0.5 % BSA) and resuspended in the same buffer and kept on ice. Half the cells were transferred to new tubes with same labels but with the addition of "37 °C". The tubes with "37 °C" were incubated at 37 °C for 60 minutes, and the "4 °C" tubes stayed on ice for 60 minutes. After 60 minutes, the "37 °C" tubes were put on ice for 15 minutes to stop internalization. All tubes were washed in buffer 2 (PBS + 0.5 % BSA + 0.01 % sodium azide) and prepared for analysis with confocal microscopy and flow cytometry. Internalization was quantified by subtracting the control (IgG) MFI from the antibody (CD11c clone BU15 or 3.9) MFI and internalization percentages were calculated.

4 Results

4.1 Gating

Gating of cell populations was done manually and following the usual procedures at the Laboratory of Immunology at Aalborg University.

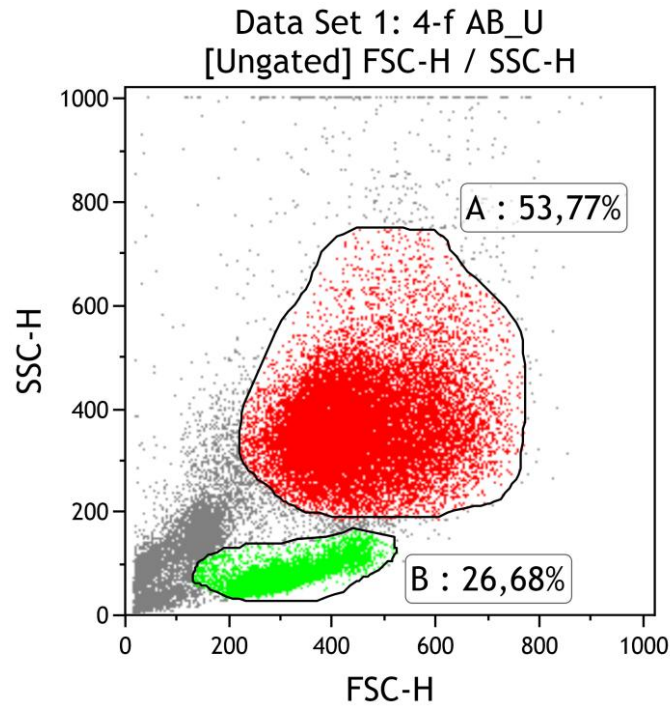


Figure 4.1. Gating for cell populations. Gate A represents the anticipated DC population, gate B represents the anticipated B- and T cell population. X-axis represents forward scatter height (FSC-H), Y-axis represents side scatter height (SSC-H).

Flow cytometric data processing involved gating of various anticipated cell populations in forward scatter (FSC) and side scatter (SSC) dot plots. Samples were gated manually and identically within and between experiments if possible. Gate placement varied slightly depending on the maturity level of DCs. Figure 4.1 illustrates typical gates for DC and lymphocyte populations. DC populations typically varied between 40-75 % of total events in all experiments.

4.2 Controls

4.2.1 Isotype control

DCs and monocytes carry several types of Fc receptors. Therefore, it is important to include isotype controls to separate FcR-mediated binding from specific binding.

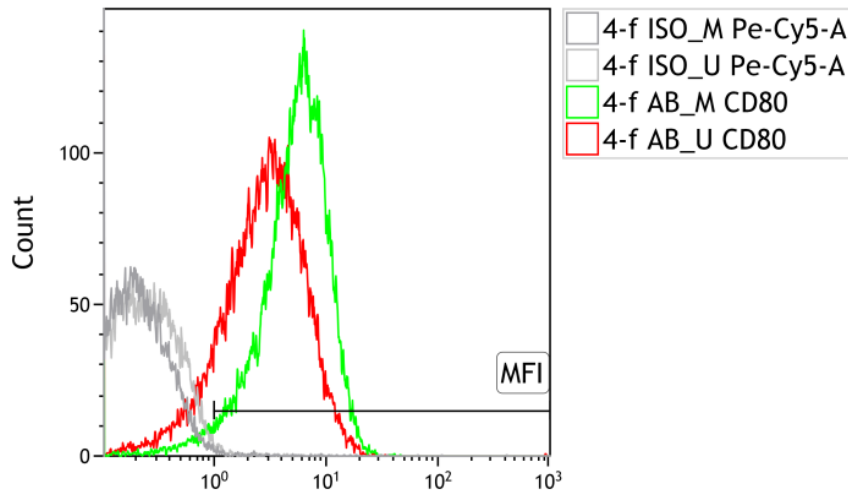


Figure 4.2. Typical isotype control. Green and red graphs represents the antibodies for CD80-PE-Cy5 on two different DC populations (mature and immature), grey and light grey graphs represents the corresponding IgG1,k-PE-Cy5 isotype for each sample. Histogram: The y-axis represents the cell count, x-axis represents fluorescence intensity for CD80-PE-Cy5.

Isotypes were included for each sample to analyze the non-specific Fc binding of antibodies for each individual sample. Isotype peaks were adjusted to be placed at less than 10^0 fluorescence intensity in the FACSDiva program. Thus, the MFI was calculated based on specific binding as the fluorescence intensity above 10^0 . Figure 4.2 illustrates a CD80-PE-Cy5 antibody with the corresponding isotype IgG1,k-PE-Cy5 that is located on the histogram below 10^0 fluorescence intensity.

4.2.2 Doublet control

Doublets can occur in flow cytometric analyses, resulting in unreliable fluorescence measurements, and therefore it is important to correct and remove any doublets in samples.

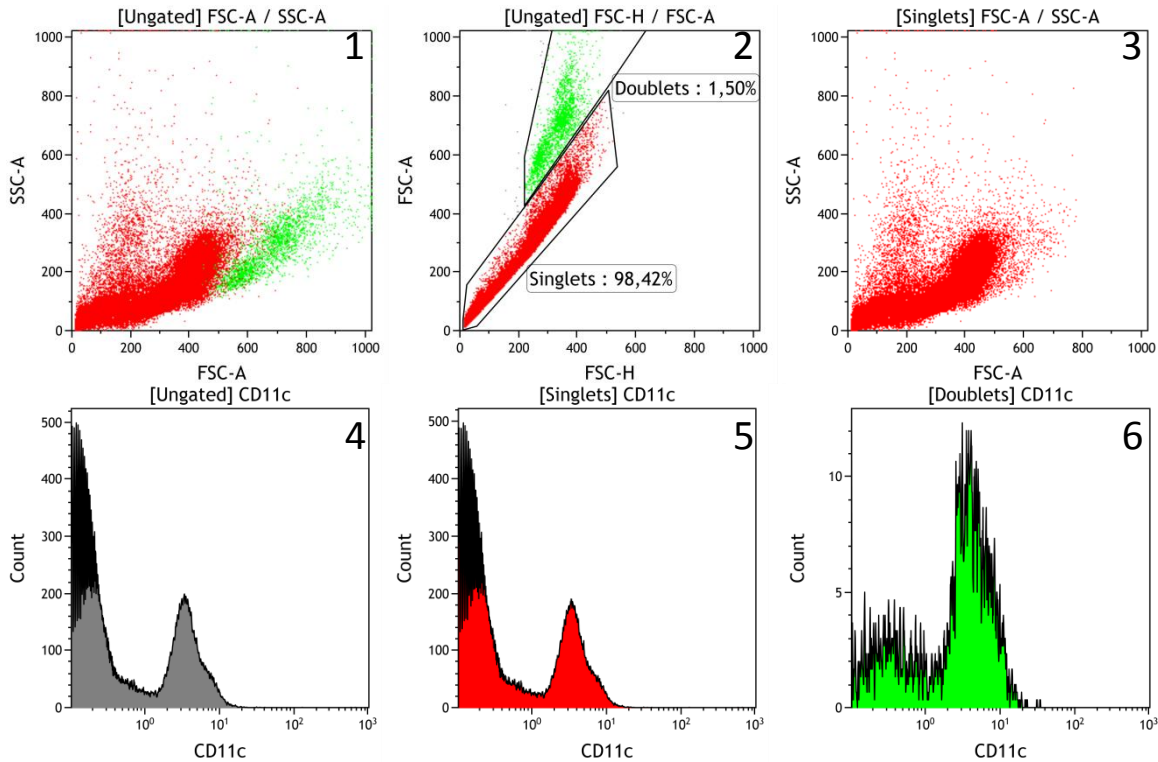


Figure 4.3. Example of a doublet control on a PBMC sample. The first SSC-A/FSC-A dot plot represents the normal illustration of the population, and the FSC-A/FSC-H illustrates the repeated population high on the FSC-A axis. The last SSC-A/FSC-A dot plot represents the singlet population with all doublets removed. Dot plots 1 and 3: The y-axis represents side scatter area (SSC-A), x-axis represents the forward scatter area (FSC-A). Dot plot 2: The y-axis represents the forward scatter area (FSC-A), x-axis represents the forward scatter height (FSC-H). Histograms: The y-axis represents the cell count, x-axis represents fluorescence intensity for CD11c-PE in ungated, singlet gated and doublet gated populations.

Doublets were corrected for when present by analyzing the sample in a FSC-A and FSC-H dot plot and gating the singlet population following the X-Y-axis, and removing any cells that creates a similar population higher up on the FSC-A axis as seen in figure 4.3. Doublets did not affect the fluorescence signal by a substantial amount. Doublet percentages were no higher than 4 % and on average lower than 1 % for all samples. High doublet percentages over 2 % were only observed in samples with whole blood and PBMCs.

4.2.3 Lymphocyte control

Lymphocytes can occur in samples that were not sufficiently purified, and it is important to analyze the percentages due to the possible activating effect that T cells can have on DCs.

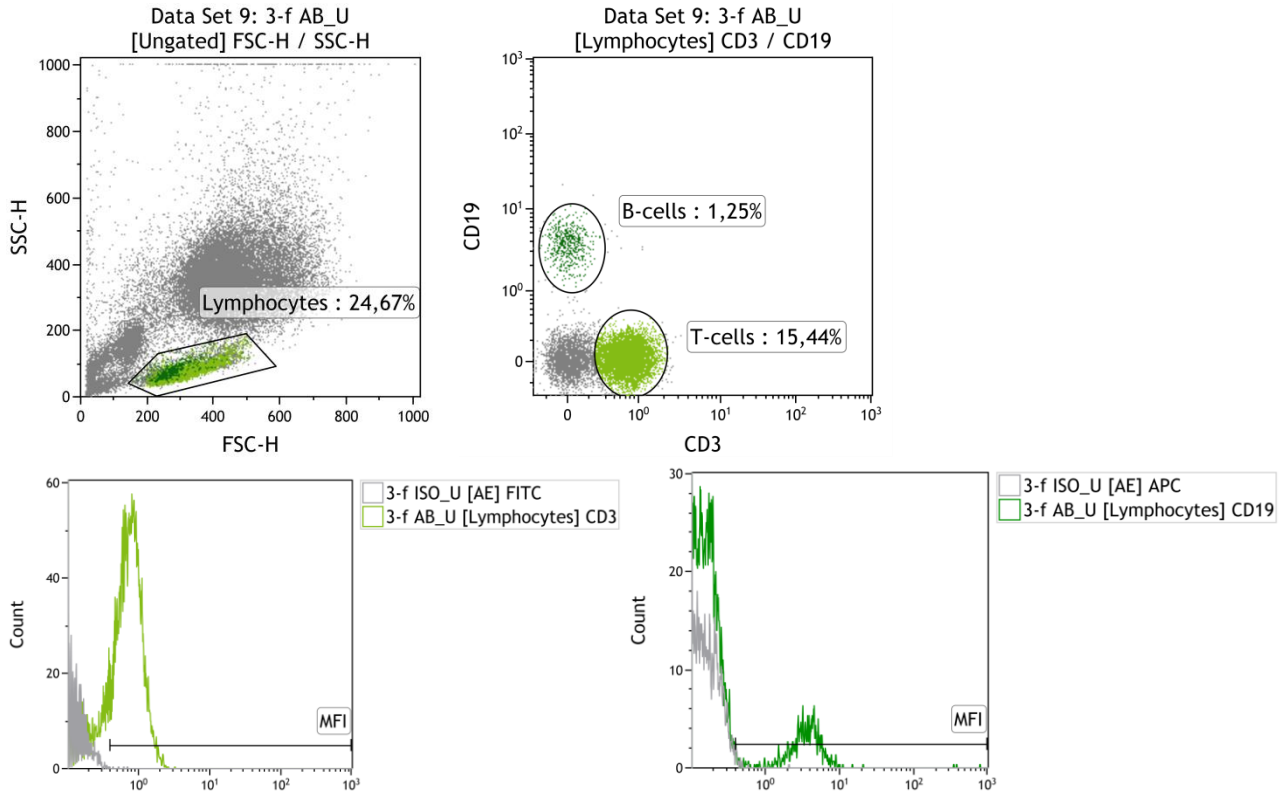


Figure 4.4. Stain for CD3 for T cells and CD19 for B cells. Dot plots: The y-axis represents side scatter height (SSC-H) and CD19 for the gated lymphocyte population, x-axis represents the forward scatter height (FSC-H) and CD3 for the gated lymphocyte population. Histograms: The y-axis represents the cell count, x-axis represents fluorescence intensity for respectively: CD3-FITC and CD19-APC. Corresponding isotypes were used; IgG2a,k-FITC and IgG1,k-APC (grey graphs).

A staining for B- and T cells in a sample of immature DCs is illustrated in figure 4.4. Lymphocyte populations were gated as a population low on the SSC axis in accordance with the low granulation of lymphocytes, also lower on the FSC axis compared to DCs due to their smaller size. The lymphocyte populations were then analyzed in CD19/CD3 dot plots to determine the percentage of B- and T cells. CD19 is a lineage marker for B cells, CD3 is a lineage marker for T cells. Lymphocyte percentages were generally below 20 % for each sample, with B cells lower than 2 % and T cells lower than 16 %.

4.2.4 Monocyte control

Monocytes can occur in samples if they didn't differentiate into DCs, and therefore it is important to analyze the percentage of monocytes in order to know if some very unable to differentiate.

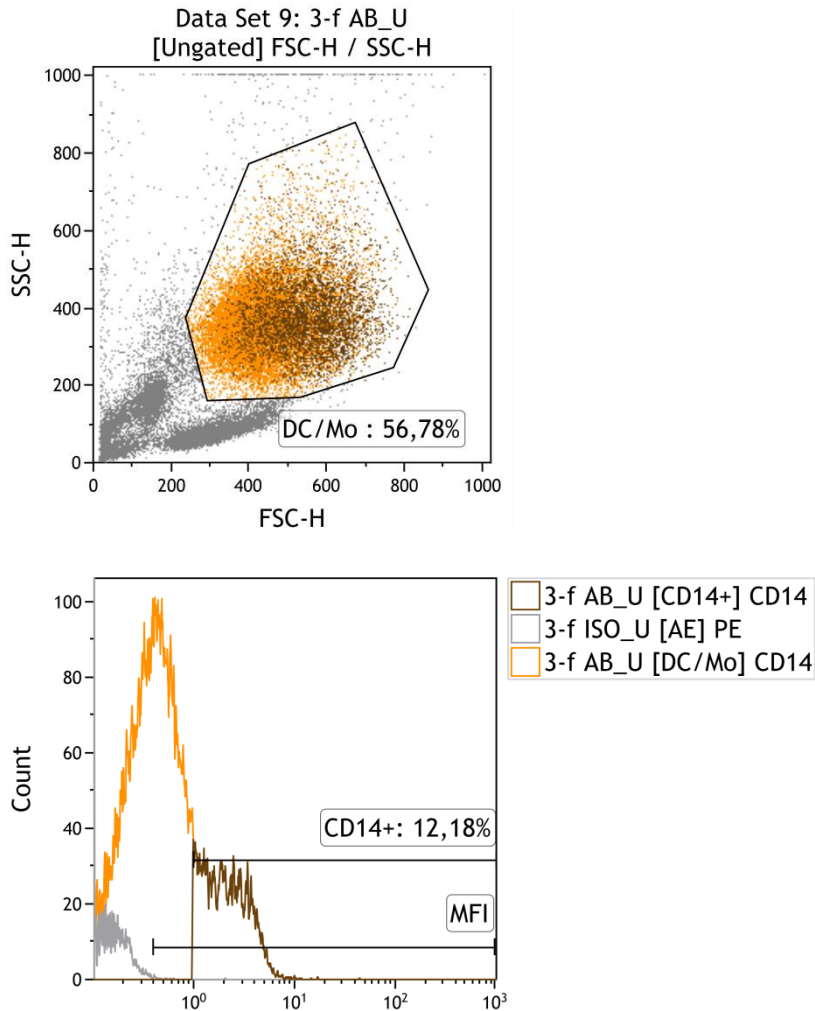


Figure 4.5. CD14 stain for monocytes. Dot plots: The y-axis represents side scatter height (SSC-H), x-axis represents the forward scatter height (FSC-H). Histograms: The y-axis represents the cell count, x-axis represents fluorescence intensity for CD14-PE. Corresponding isotype was used; IgG1,k-PE.

A staining for CD14⁺ monocytes was made for each sample to analyze the presence of monocytes in early experiments. This control was only performed in pilot and early experiments to ensure the isolation and differentiation of monocytes to DCs worked as expected. An example from an early experiment is illustrated in figure 4.5, where CD14⁺ cells represents 12,18 % of all events in the sample which was typical for most samples.

4.3 Pilot experiments

4.3.1 Separation of immature and mature populations

To prepare for the main experiments a pilot experiment was performed to make sure that it was possible to differentiate between a mature and immature in an established DC population. This was important to know before investigating if CD11c antibodies could induce maturation in DCs.

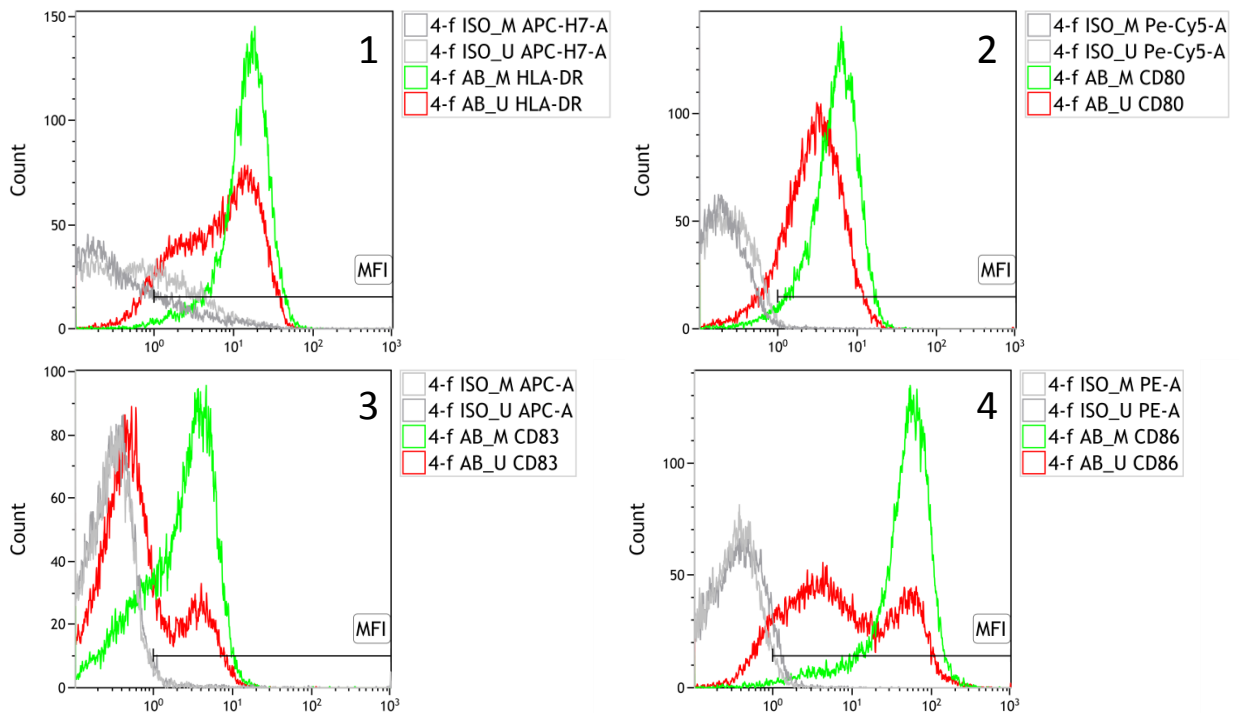


Figure 4.6. Typical example of the expression of HLA-DR, CD80, CD83 and CD86 on DCs. DCs cultured with LPS (green) and without LPS (red) and corresponding isotypes (light, medium and dark grey). DCs were incubated with LPS for 24 hours before harvesting. Histograms: The y-axis represents the cell count, x-axis represents fluorescence intensity. Histogram 1: HLA-DR-APC-H7 and isotype IgG2a,k-APC-H7. Histogram 2: CD80-Pe-Cy5 and isotype IgG1,k-Pe-Cy5. Histogram 3: CD83-APC and isotype IgG1,k-APC. Histogram 4: CD86-PE and isotype IgG1,k-PE.

MFI (mean fluorescence intensity):

Mature: HLA-DR (15,91), CD80 (5,45), CD83 (3,34), CD86 (42,10)

Immature: HLA-DR (13,87), CD80 (3,38), CD83 (3,00), CD86 (12,28)

This is a typical result illustrated from one out of two similar experiments. Raw data and controls for the samples illustrated can be found in appendix 8.2.4.

Figure 4.6 illustrates the expression of DC maturation markers on 2 DC populations; one unstimulated (immature) and one stimulated (mature) with LPS 24 hours before harvest and analysis. The immature DCs express low levels of HLA-DR, CD83 and CD86 but with small peaks in higher fluorescence intensity, indicating that part of the population is mature. CD80 is approximately the same as the mature population. The mature DCs express much more HLA-DR, CD83 and CD86 compared to the immature population.

4.3.2 Morphology of immature and mature moDCs

The morphology of immature and mature populations was assessed to visually determine the maturity level of the cells.

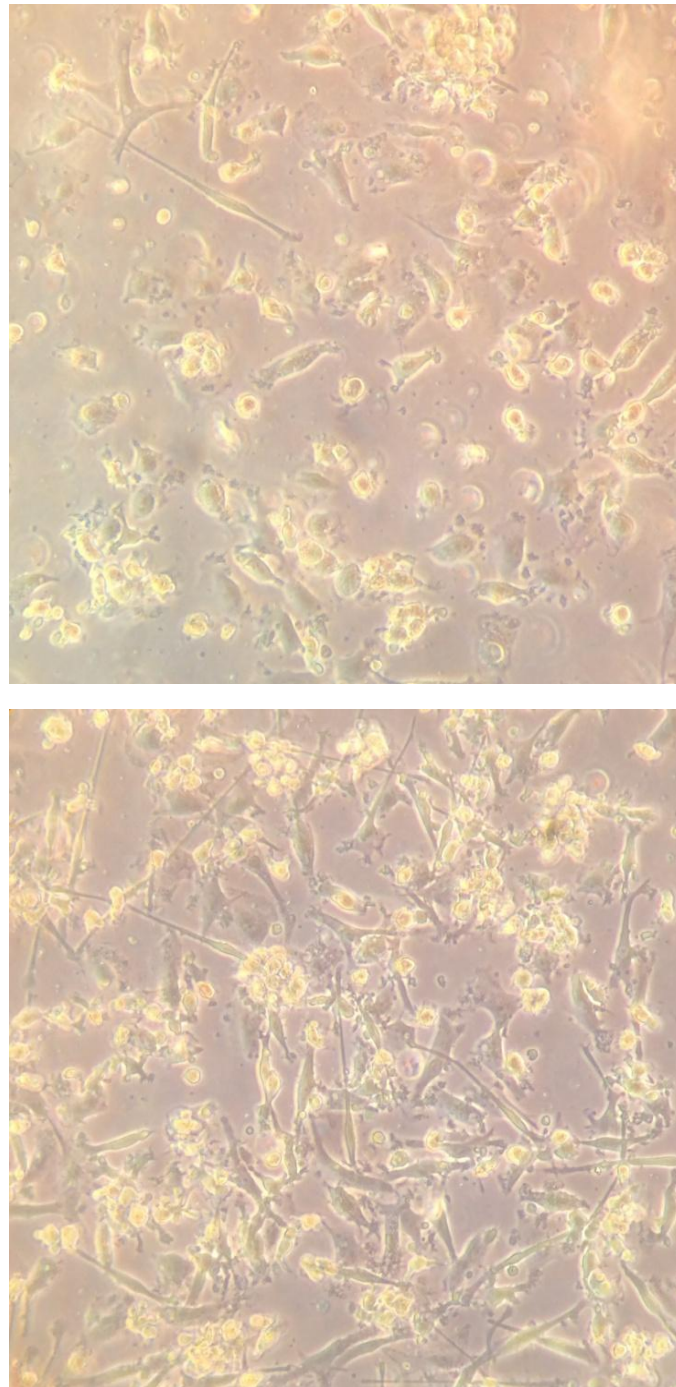


Figure 4.7. Phase contrast microscopy images (20x objective) of immature (top image) and mature (bottom image) DC populations. Raw data can be found in appendix 8.2.3.

Figure 4.7 illustrates the difference in morphology between an immature and mature DC population. Immature DCs are round and have few veils and dendrites. Mature DCs have more veils and multiple dendrites with a many more varied shapes and forms compared to the immature DCs.

4.3.3 Optimization of isolation kit

To ensure high purity of monocytes and differentiated DCs thereof, two different monocyte isolation kits were tested, a positive (CD14⁺ kit) and a negative (Monocyte Isolation Kit II) isolation kit. Additionally, the ability to mature and stay immature of the DCs differentiated from the isolated monocytes was observed. The positive isolation kit works by isolating and collecting the CD14 positive cells, and the negative isolation kit works by isolating all other cells but monocytes, which are then collected.

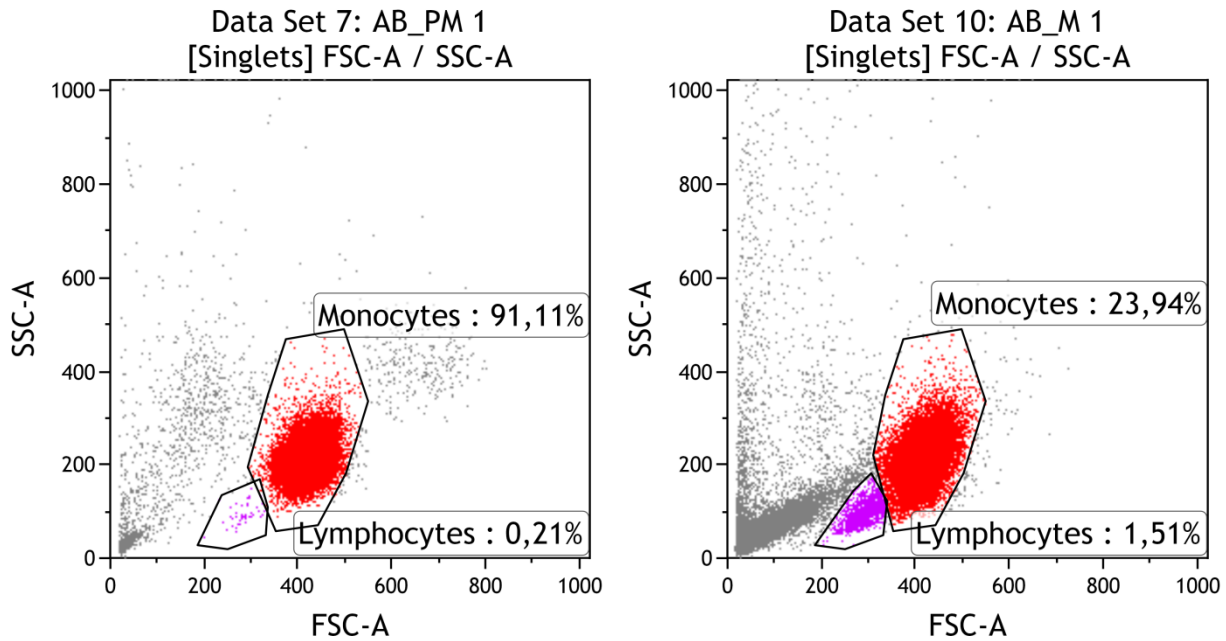


Figure 4.7. Purity of positive and negative isolated monocytes. The left SSC-A/FSC-A dot plot represents a monocyte population that was isolated with a positive kit (CD14⁺ kit). The right SSC-A/FSC-A dot plot represents a monocyte population that was isolated with a negative isolation kit (Monocyte Isolation Kit II). Dot plots: The y-axis represents side scatter area (SSC-A), x-axis represents the forward scatter area (FSC-A).

Figure 4.7 illustrates the monocyte populations after isolating with either a positive or negative monocyte isolation kit. The monocyte population from the positive isolation kit is very pure with 91,11 % monocytes and 0,21 % lymphocytes. The monocyte population from the negative isolation kit is less pure with 23,94 % monocytes and 1,51 % lymphocytes. The percentages missing from each kit is debris and other cells.

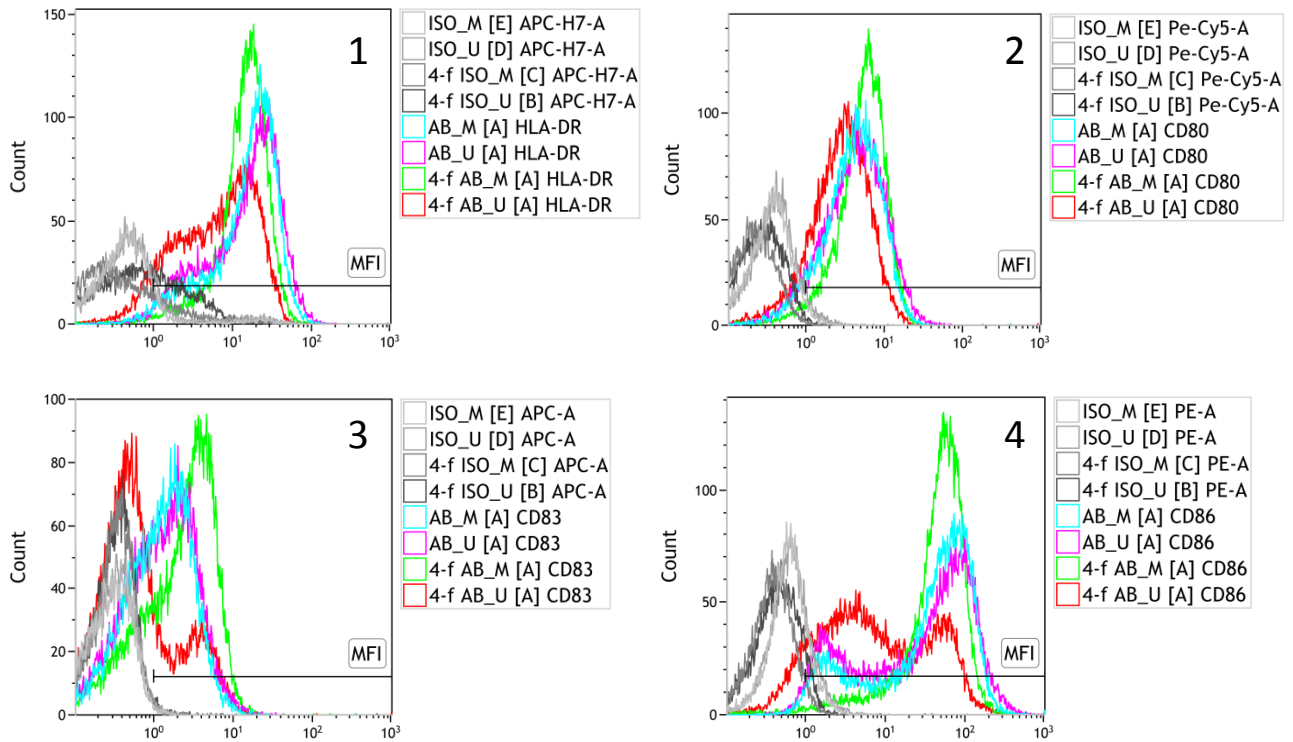


Figure 4.8. Expression of HLA-DR, CD80, CD83 and CD86 on DCs differentiated from monocytes isolated with 2 different isolation kits. DCs from CD14⁺ kit (positive) matured with LPS (turquoise), DCs from CD14⁺ kit (positive) without LPS (pink), DCs from Monocyte Isolation Kit II (negative) matured with LPS (green), DCs from Monocyte Isolation Kit II (negative) without LPS (red) and corresponding isotypes (light, medium, dark and very dark grey). DCs were incubated with LPS for 24 hours before harvesting. Histograms: The y-axis represents the cell count, x-axis represents fluorescence intensity. Histogram 1: HLA-DR-APC-H7 and isotype IgG2a,k-APC-H7. Histogram 2: CD80-Pe-Cy5 and isotype IgG1,k-Pe-Cy5. Histogram 3: CD83-APC and isotype IgG1,k-APC. Histogram 4: CD86-PE and isotype IgG1,k-PE.

MFI:

CD14⁺ mature: HLA-DR (14,58), CD80 (4,47), CD83 (2,19), CD86 (30,63)

CD14⁺ immature: HLA-DR (14,18), CD80 (4,77), CD83 (2,40), CD86 (24,57)

Negative isolation kit mature: HLA-DR (1), CD80 (5,43), CD83 (3,30), CD86 (42,08)

Negative isolation kit immature: HLA-DR (7,16), CD80 (3,35), CD83 (2,92), CD86 (9,83)

Raw data and controls for the samples illustrated can be found in appendix 8.2.4 and 8.2.6.

Figure 4.8 illustrates the expression of maturation markers on DC populations that were differentiated from 2 differently isolated monocytes. DCs differentiated from monocytes isolated with the CD14⁺ kit showed a high expression of HLA-DR, CD80, CD83 and CD86 regardless of whether they were stimulated with LPS or not. DCs differentiated from monocytes isolated negatively with the Monocyte Isolation Kit II showed maturation after being stimulated with LPS and the population without LPS remained immature.

4.3.4 Optimization of columns

To ensure high purity of monocytes and differentiated DCs thereof, two different columns were tested for the negative isolation kit, Monocyte Isolation Kit II.

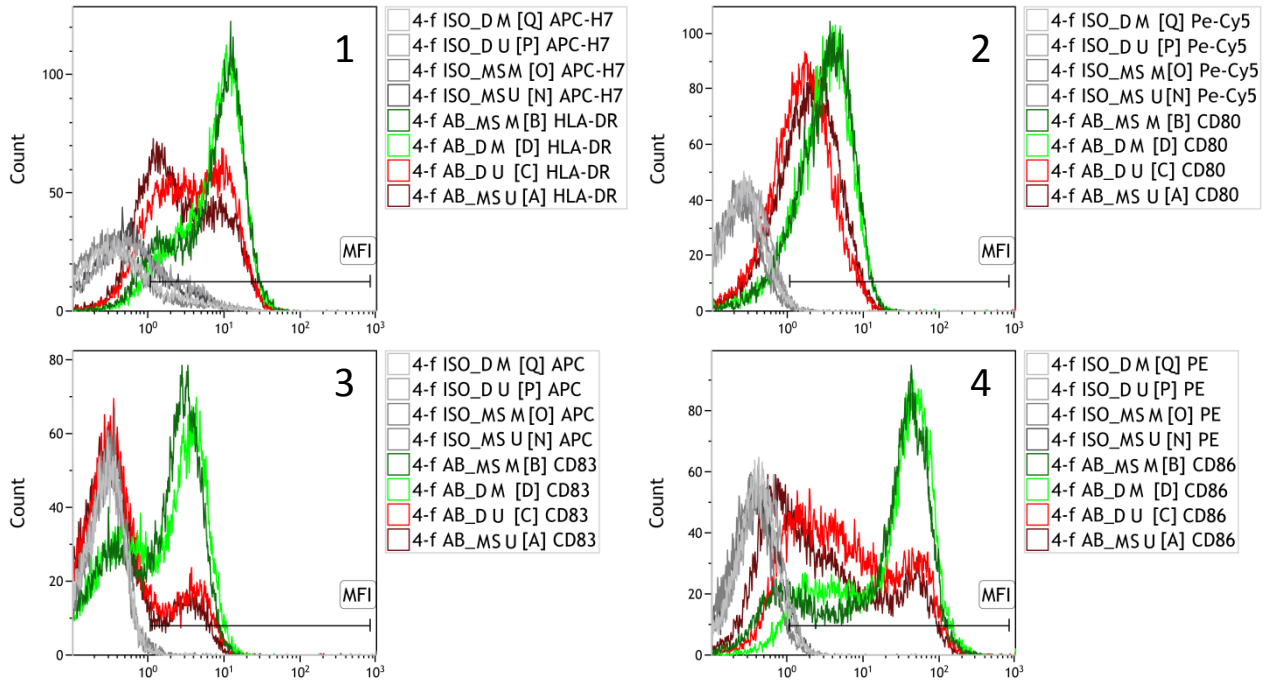


Figure 4.9. Expression of HLA-DR, CD80, CD83 and CD86 on DCs differentiated from monocytes separated in 2 different columns. D column DCs matured with LPS (green), D column DCs without LPS (red), MS column DCs matured with LPS (dark green), MS column DCs without LPS (dark red) and corresponding isotypes (light, medium, dark and very dark grey). DCs were incubated with LPS for 24 hours before harvesting. Histograms: The y-axis represents the cell count, x-axis represents fluorescence intensity. Histogram 1: HLA-DR-APC-H7 and isotype IgG2a,k-APC-H7. Histogram 2: CD80-Pe-Cy5 and isotype IgG1,k-Pe-Cy5. Histogram 3: CD83-APC and isotype IgG1,k-APC. Histogram 4: CD86-PE and isotype IgG1,k-PE.

MFI:

D column mature: HLA-DR (7,45), CD80 (3,57), CD83 (3,31), CD86 (21,71)

D column immature: HLA-DR (4,73), CD80 (2,38), CD83 (3,12), CD86 (8,24)

MS column mature: HLA-DR (7,54), CD80 (3,66), CD83 (2,93), CD86 (22,22)

MS column immature: HLA-DR (5,06), CD80 (2,68), CD83 (2,96), CD86 (7,42)

Raw data and controls for the samples illustrated can be found in appendix 8.2.3.

Figure 4.9 illustrated the expression of maturation markers for DC population that were differentiated from monocytes isolated with Monocyte Isolation Kit II with 2 different column types. There is no significant difference between column MS and D in regards to maturation of unstimulated or LPS stimulated DC populations.

4.4 CD11c distribution

4.4.1 CD11c distribution in whole blood

The distribution of CD11c was investigated on whole blood samples to see what populations expressed the molecule.

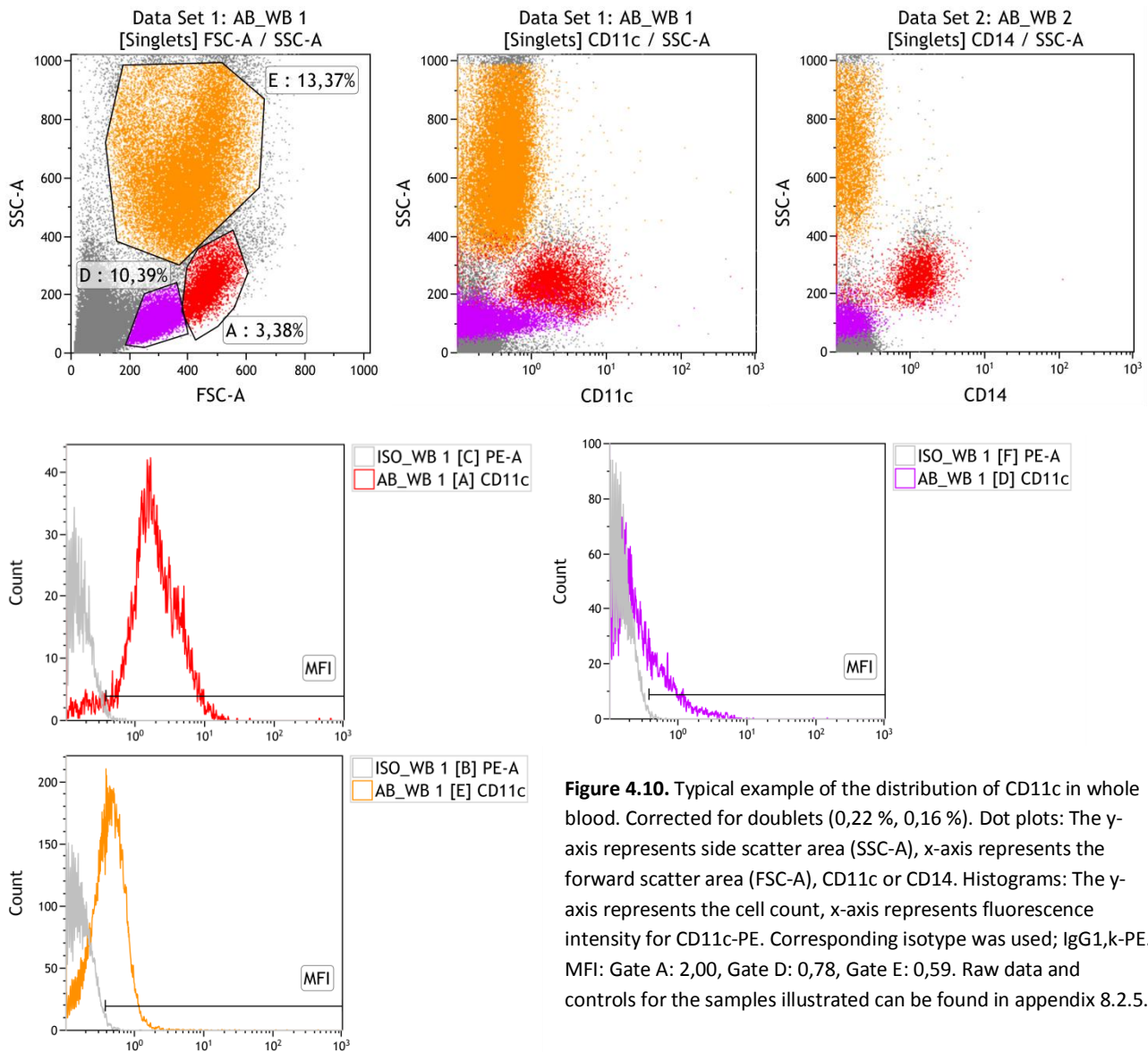


Figure 4.10 illustrates the distribution of CD11c in whole blood samples. The suspected monocyte and DC population (A) is positive for both CD11c and CD14 as seen in the SSC-A / CD11c and SSC-A / CD14 dot plots. A fraction of the cells in gate E is positive for CD11c as well.

4.4.2 CD11c distribution in PBMCs

The distribution of CD11c was investigated on PBMC samples to see what populations expressed the molecule.

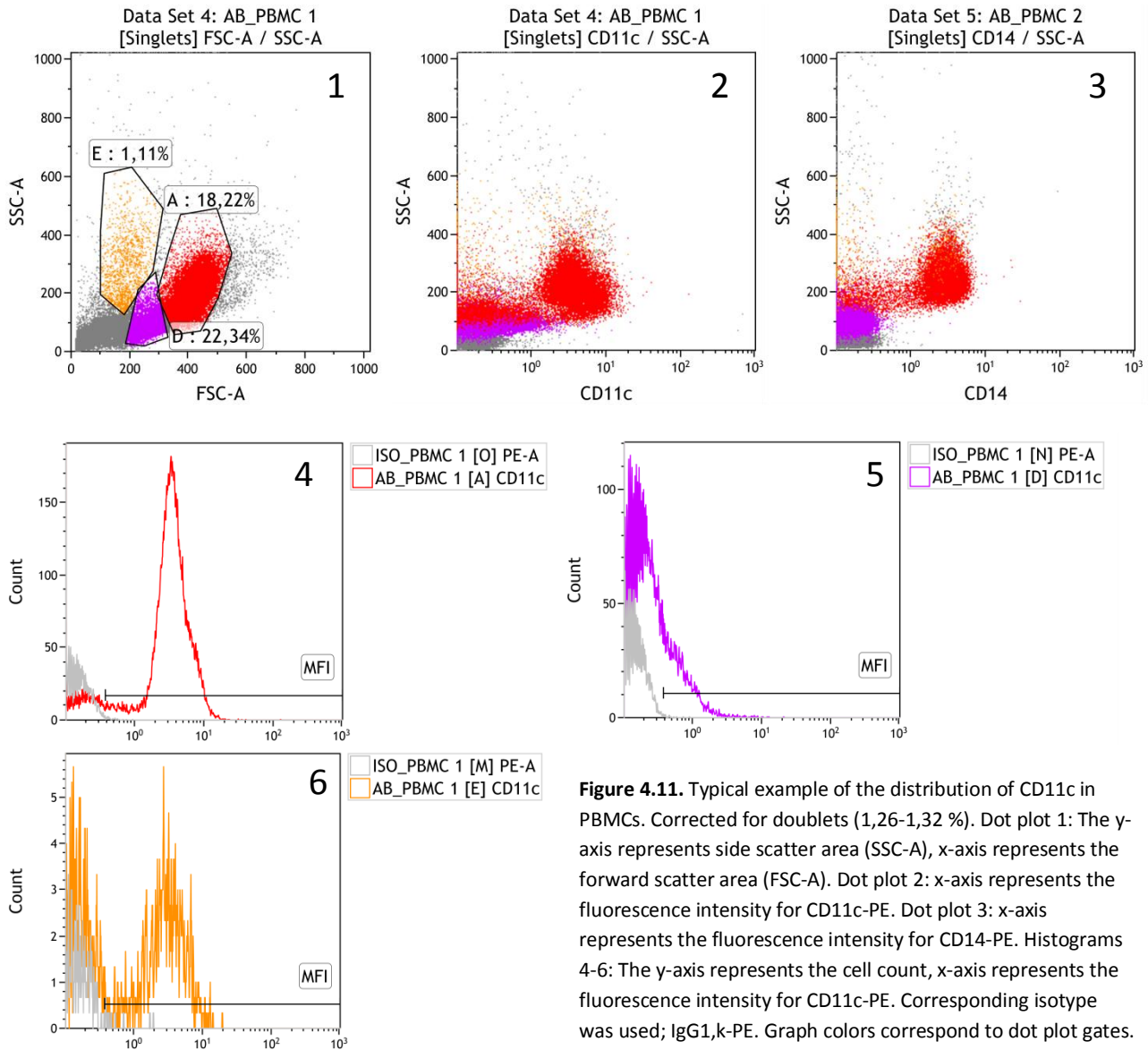


Figure 4.11. Typical example of the distribution of CD11c in PBMCs. Corrected for doublets (1,26-1,32 %). Dot plot 1: The y-axis represents side scatter area (SSC-A), x-axis represents the forward scatter area (FSC-A). Dot plot 2: x-axis represents the fluorescence intensity for CD11c-PE. Dot plot 3: x-axis represents the fluorescence intensity for CD14-PE. Histograms 4-6: The y-axis represents the cell count, x-axis represents the fluorescence intensity for CD11c-PE. Corresponding isotype was used; IgG1,k-PE. Graph colors correspond to dot plot gates. MFI: Gate A: 3,39, Gate D: 0,69, Gate E: 2,70. Raw data and controls for the samples illustrated can be found in appendix 8.2.5.

Figure 4.11 illustrates the distribution of CD11c in PBMC samples. The monocyte and DC population (A) is positive for both CD11c and CD14 as seen in the SSC-A / CD11c and SSC-A / CD14 dot plots. A small fraction of cells in gate D and E is positive for CD11c as well.

4.4.3 CD11c distribution in PBMCs analyzed on a cell sorter

The distribution of CD11c was investigated on PBMC samples to see what populations expressed the molecule in relation to CD14 and HLA-DR.

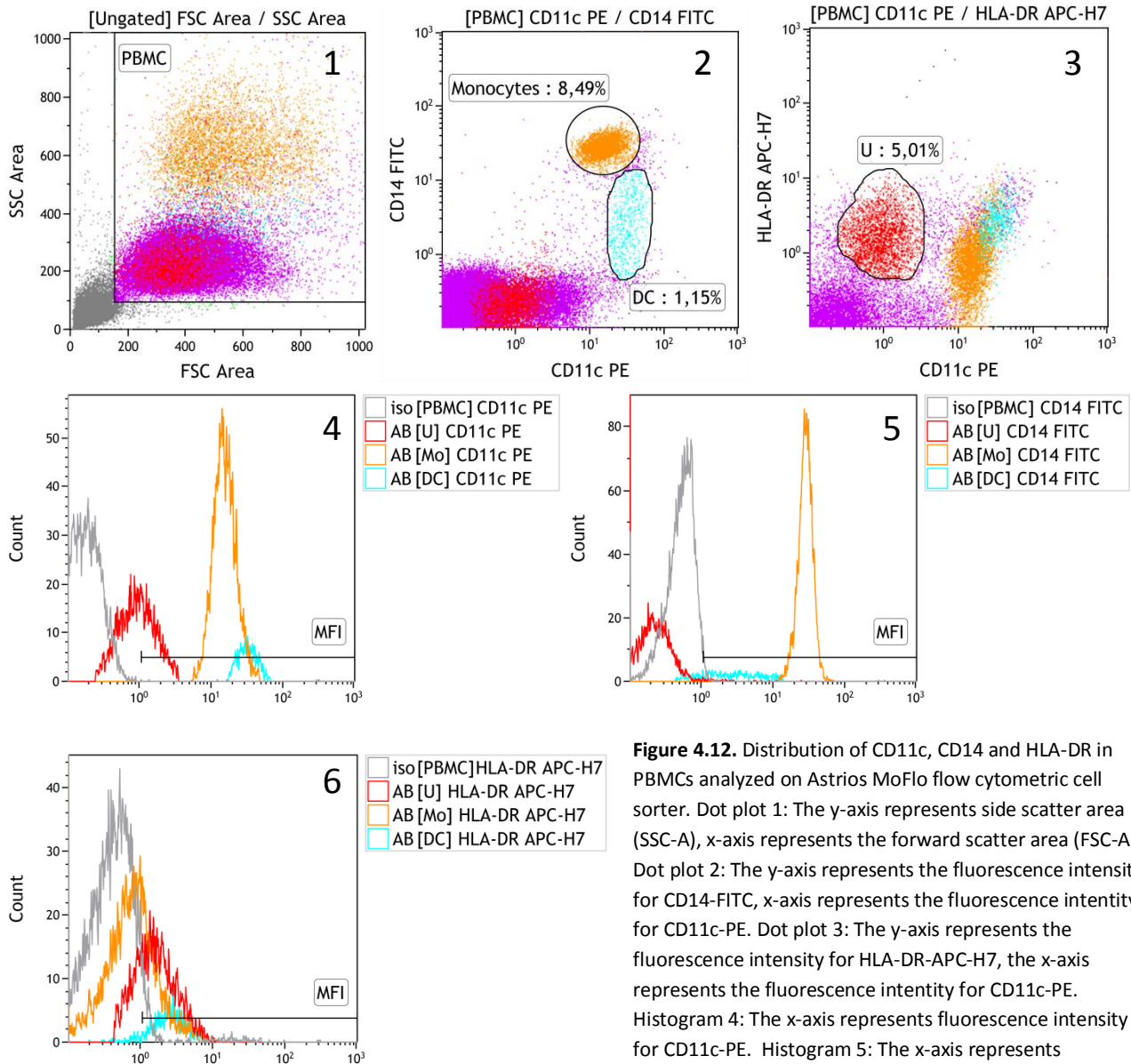


Figure 4.12. Distribution of CD11c, CD14 and HLA-DR in PBMCs analyzed on Astrios MoFlo flow cytometric cell sorter. Dot plot 1: The y-axis represents side scatter area (SSC-A), x-axis represents the forward scatter area (FSC-A). Dot plot 2: The y-axis represents the fluorescence intensity for CD14-FITC, x-axis represents the fluorescence intensity for CD11c-PE. Dot plot 3: The y-axis represents the fluorescence intensity for HLA-DR-APC-H7, the x-axis represents the fluorescence intensity for CD11c-PE. Histogram 4: The x-axis represents fluorescence intensity for CD11c-PE. Histogram 5: The x-axis represents

fluorescence intensity for CD14-FITC. Histogram 6: The x-axis represents fluorescence intensity for HLA-DR-APC-H7. Corresponding isotypes were used; IgG1,k-PE, IgG1,k-FITC and IgG2a,k-APC-H7. Graph colors correspond to dot plot gates.

MFI: Gate DC: CD11c (32,40), CD14 (3,48), HLA-DR (2,72). Gate Monocytes: CD11c (15,52), CD14 (28,43), HLA-DR (1,83). Gate U: CD11c (1,62), CD14 (2,13), HLA-DR (2,17).

Figure 4.12 illustrates the distribution of CD11c, CD14 and HLA-DR in a PBMC population analyzed on a cell sorting device. The DC population is very positive for CD11c, and some are positive for CD14 as well. The monocyte population is positive for CD11c as well, although not as much as the DC population. An unknown cell population (gate U) expresses CD11c in very small amounts as well, but is negative for CD14. All 3 populations are positive for HLA-DR.

4.4.4 CD11c distribution in negative isolated monocytes

The distribution of CD11c was investigated on negative isolated monocyte samples to see what populations expressed the molecule.

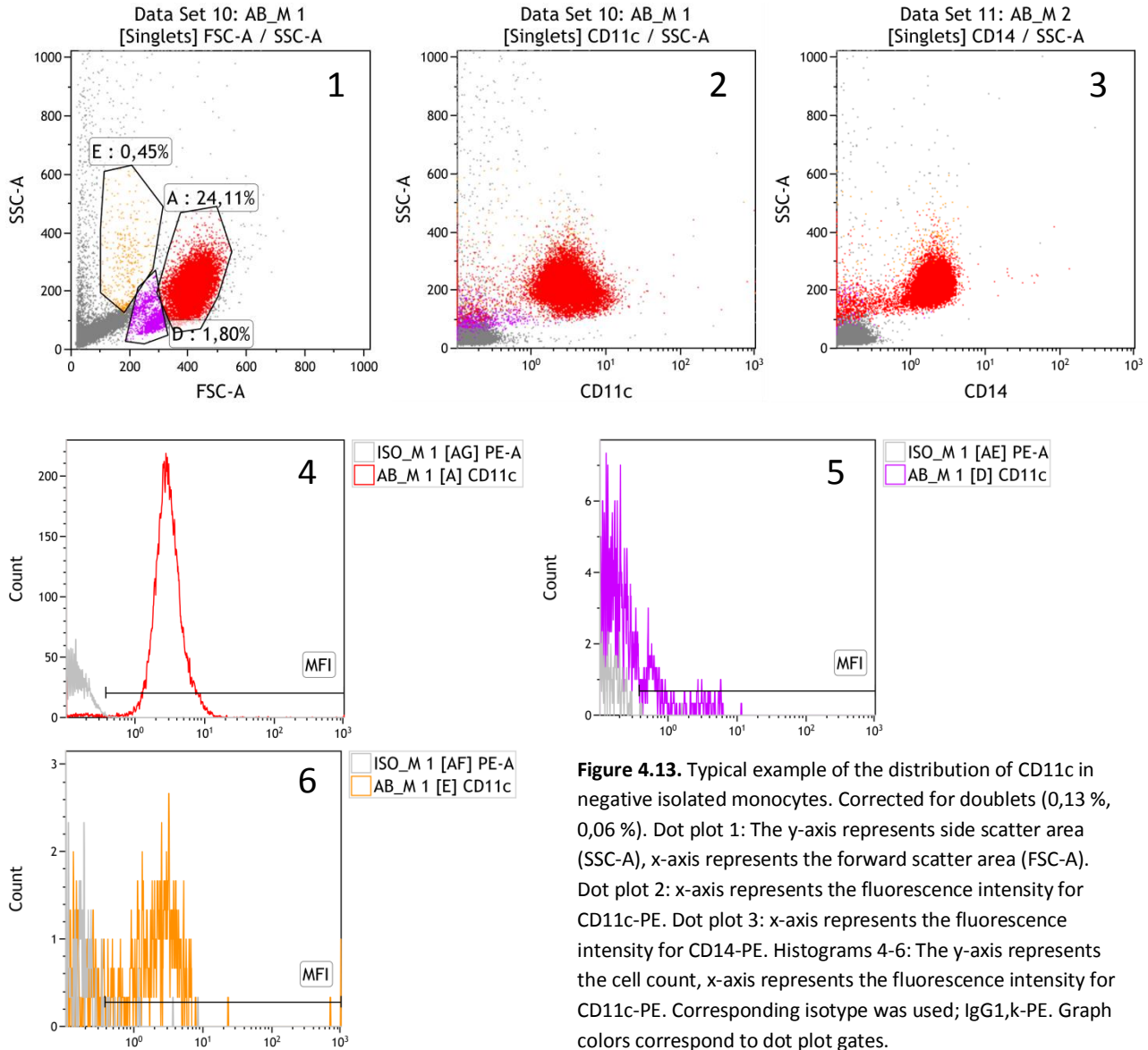


Figure 4.13. Typical example of the distribution of CD11c in negative isolated monocytes. Corrected for doublets (0,13 %, 0,06 %). Dot plot 1: The y-axis represents side scatter area (SSC-A), x-axis represents the forward scatter area (FSC-A). Dot plot 2: x-axis represents the fluorescence intensity for CD11c-PE. Dot plot 3: x-axis represents the fluorescence intensity for CD14-PE. Histograms 4-6: The y-axis represents the cell count, x-axis represents the fluorescence intensity for CD11c-PE. Corresponding isotype was used; IgG1,k-PE. Graph colors correspond to dot plot gates. MFI: Gate A: 2,98, Gate D: 1,03, Gate E: 2,18. Raw data and controls for the samples illustrated can be found in appendix 8.2.5.

Figure 4.13 illustrates the distribution of CD11c in samples with monocytes isolated with Monocyte Isolation Kit II. The suspected monocyte population (A) is positive for both CD11c and CD14 as seen in the SSC-A / CD11c and SSC-A / CD14 dot plots. A very small fraction of cells in gate D and E is positive for CD11c as well.

4.4.5 CD11c distribution in positive isolated monocytes

The distribution of CD11c was investigated on positive isolated monocyte samples to see what populations expressed the molecule.

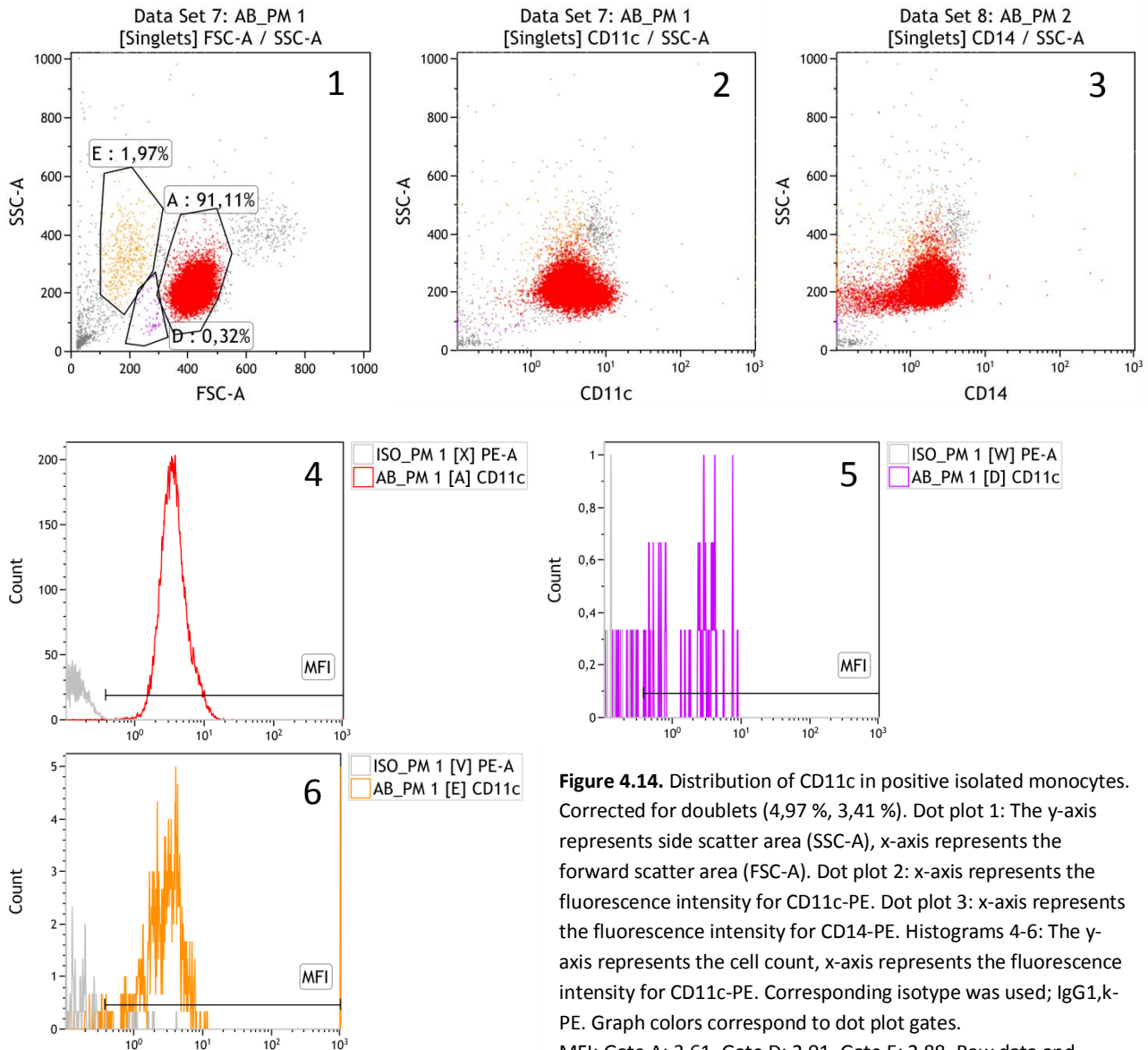


Figure 4.14. Distribution of CD11c in positive isolated monocytes. Corrected for doublets (4,97 %, 3,41 %). Dot plot 1: The y-axis represents side scatter area (SSC-A), x-axis represents the forward scatter area (FSC-A). Dot plot 2: x-axis represents the fluorescence intensity for CD11c-PE. Dot plot 3: x-axis represents the fluorescence intensity for CD14-PE. Histograms 4-6: The y-axis represents the cell count, x-axis represents the fluorescence intensity for CD11c-PE. Corresponding isotype was used; IgG1,k-PE. Graph colors correspond to dot plot gates. MFI: Gate A: 3,61, Gate D: 2,01, Gate E: 2,88. Raw data and controls for the samples illustrated can be found in appendix 8.2.5.

Figure 4.14 illustrates the distribution of CD11c in samples with monocyte isolated with a CD14⁺ kit. The suspected monocyte population (A) is positive for both CD11c and CD14 as seen in the SSC-A / CD11c and SSC-A / CD14 dot plots. A very small fraction of cells in gate D and E is positive for CD11c as well.

4.5 Maturation

4.5.1 Maturation by CD11c antibody clone 3.9

To investigate if the CD11c antibody clone 3.9 induced maturation in DC populations, 2 different concentrations of the antibody was added to the culture 24 hours prior to harvesting and analysis with 4 maturation marker stains.

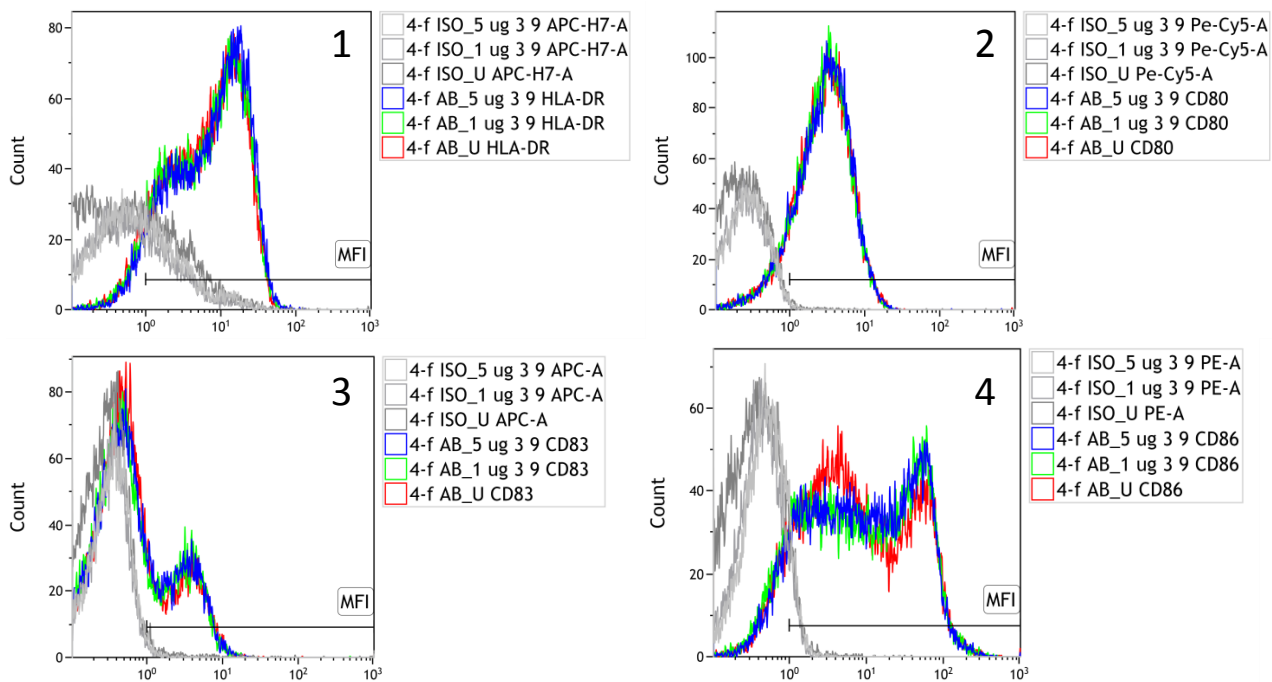


Figure 4.15. Typical example of the expression of HLA-DR, CD80, CD83 and CD86 on DCs cultured with CD11c antibody clone 3.9. DCs cultured with 1 µg/ml (green), 5 µg/ml (blue) and 0 µg/ml (red) was stained with 4 different fluorochrome conjugate antibodies with corresponding isotypes (light, medium and dark grey). DCs were incubated with CD11c antibody clone 3.9 for 24 hours before harvesting. Histograms: The y-axis represents the cell count, x-axis represents fluorescence intensity. Histogram 1: HLA-DR-APC-H7 and isotype IgG2a,k-APC-H7. Histogram 2: CD80-Pe-Cy5 and isotype IgG1,k-Pe-Cy5. Histogram 3: CD83-APC and isotype IgG1,k-APC. Histogram 4: CD86-PE and isotype IgG1,k-PE.

MFI:

0 µg/ml 3.9: HLA-DR (7,10), CD80 (3,32), CD83 (2,85), CD86 (9,70)

1 µg/ml 3.9: HLA-DR (7,25), CD80 (3,29), CD83 (2,87), CD86 (11,27)

5 µg/ml 3.9: HLA-DR (7,84), CD80 (3,38), CD83 (2,80), CD86 (11,13)

Raw data and controls for the samples illustrated can be found in appendix 8.2.4.

Figure 4.15 illustrates the expression of maturation markers in DC populations cultured with the CD11c antibody clone 3.9 in two different concentrations. There is no significant difference between culturing with 1 µg/ml and 5 µg/ml. Furthermore, there is no significant difference between the CD11c 3.9 stimulated populations and the unstimulated population, with the exception of the expression of CD86, that is very slightly higher for the CD11c 3.9 stimulated populations.

4.5.2 Maturation by CD11c antibody clone BU15

To investigate if the CD11c antibody clone BU15 induced maturation in DC populations, 2 different concentrations of the antibody was added to the culture 24 hours prior to harvesting and analysis with 4 maturation marker stains.

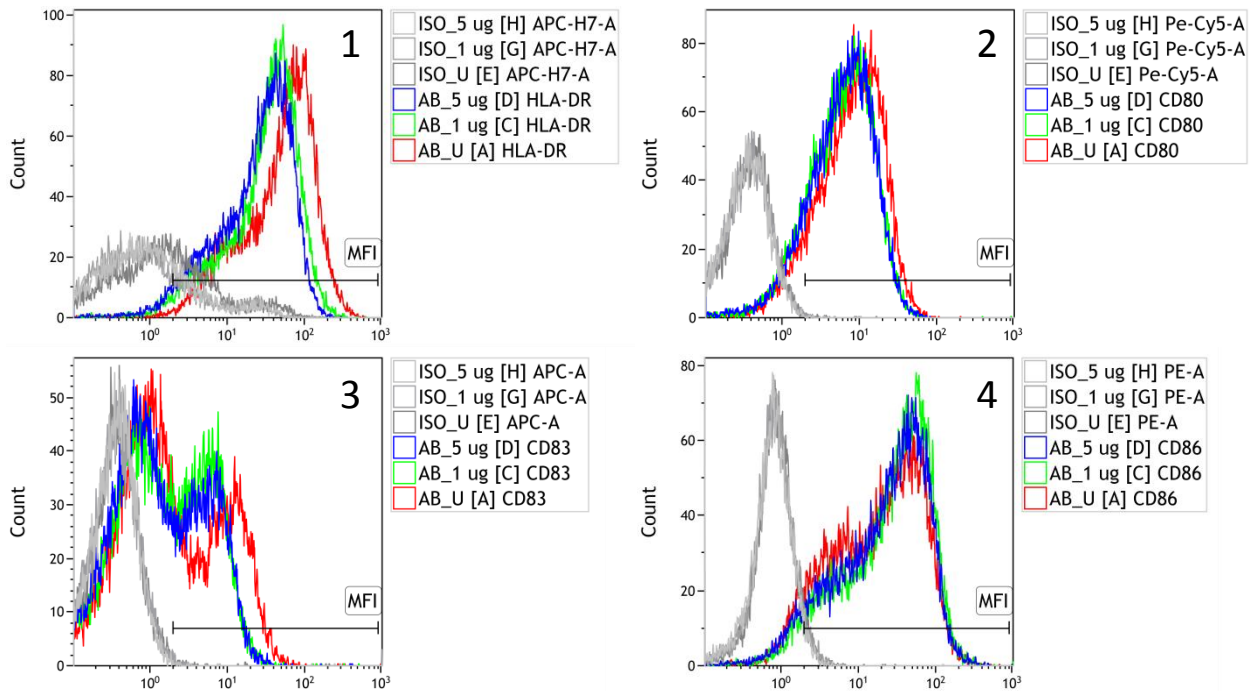


Figure 4.16. Typical example of the expression of HLA-DR, CD80, CD83 and CD86 on DCs cultured with CD11c antibody clone BU15. DCs cultured with 1 $\mu\text{g}/\text{ml}$ (green), 5 $\mu\text{g}/\text{ml}$ (blue) and 0 $\mu\text{g}/\text{ml}$ (red), corresponding was stained with 4 different fluorochrome conjugate antibodies with corresponding isotypes (light, medium and dark grey). DCs were incubated with CD11c antibody clone BU15 for 24 hours before harvesting. Histograms: The y-axis represents the cell count, x-axis represents fluorescence intensity. Histogram 1: HLA-DR-APC-H7 and isotype IgG2a,k-APC-H7. Histogram 2: CD80-Pe-Cy5 and isotype IgG1,k-Pe-Cy5. Histogram 3: CD83-APC and isotype IgG1,k-APC. Histogram 4: CD86-PE and isotype IgG1,k-PE.

MFI:

0 $\mu\text{g}/\text{ml}$ BU15: HLA-DR (45,44), CD80 (9,22), CD83 (7,99), CD86 (20,5)

1 $\mu\text{g}/\text{ml}$ BU15: HLA-DR (30,85), CD80 (7,48), CD83 (5,40), CD86 (27,14)

5 $\mu\text{g}/\text{ml}$ BU15: HLA-DR (24,50), CD80 (7,51), CD83 (5,55), CD86 (24,61)

Raw data and controls for the samples illustrated can be found in appendix 8.2.7

Figure 4.16 illustrates the expression of maturation markers in DC populations cultured with the CD11c antibody clone BU15 in two different concentrations. There is no significant difference between culturing with 1 $\mu\text{g}/\text{ml}$ and 5 $\mu\text{g}/\text{ml}$. Furthermore, there is no significant difference between the CD11c BU15 stimulated populations and the unstimulated population, although the CD11c BU15 stimulated populations seem to express less HLA-DR, CD80 and CD83 compared to the unstimulated population.

4.6 Internalization of CD11c

4.6.1 Confocal microscopy

Internalization was analyzed with confocal microscopy to visually determine if the CD11c antibody clones and the corresponding IgG were internalized by the DCs. Unstain and secondary antibody controls were included to determine any autofluorescence or unspecific binding of secondary antibodies.

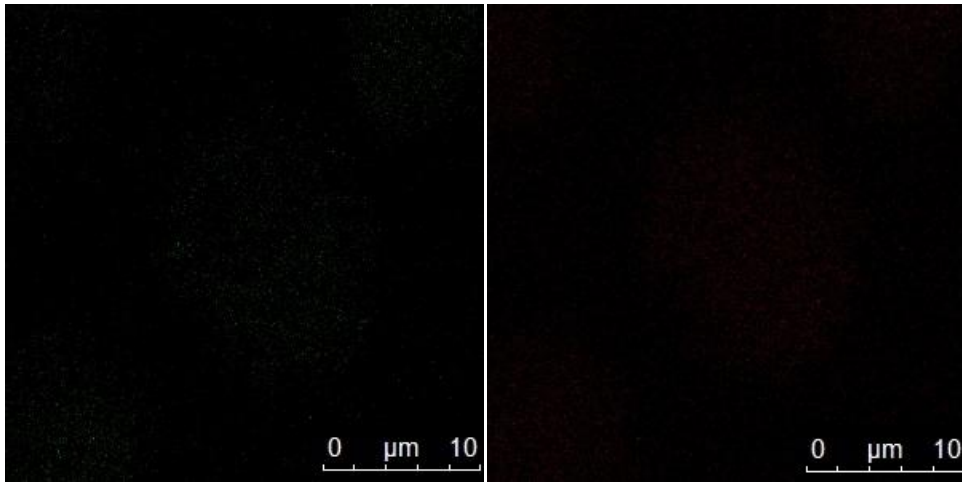


Figure 4.17. Unstain control to determine autofluorescence of cells. Left: Unstained image captured in the green channel. Right: Unstained image captured in the red channel.

Figure 4.17 illustrates an unstained sample of DCs, a control included to determine autofluorescence. Very little autofluorescence is observed.

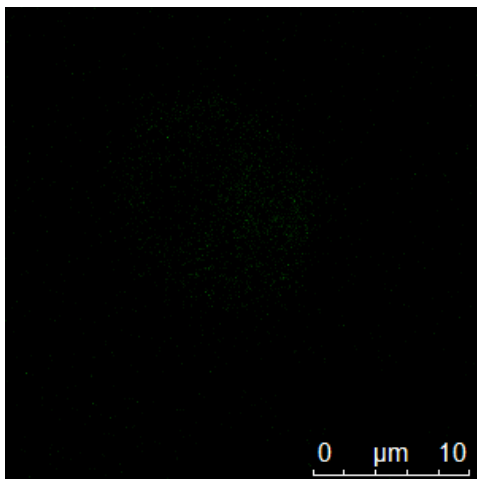


Figure 4.18. Secondary stain control to determine unspecific binding of secondary antibody, Goat-anti-mouse Alexa 488.

Figure 4.18 illustrates a secondary antibody control to determine any unspecific binding. Very little binding of the secondary antibody is observed.

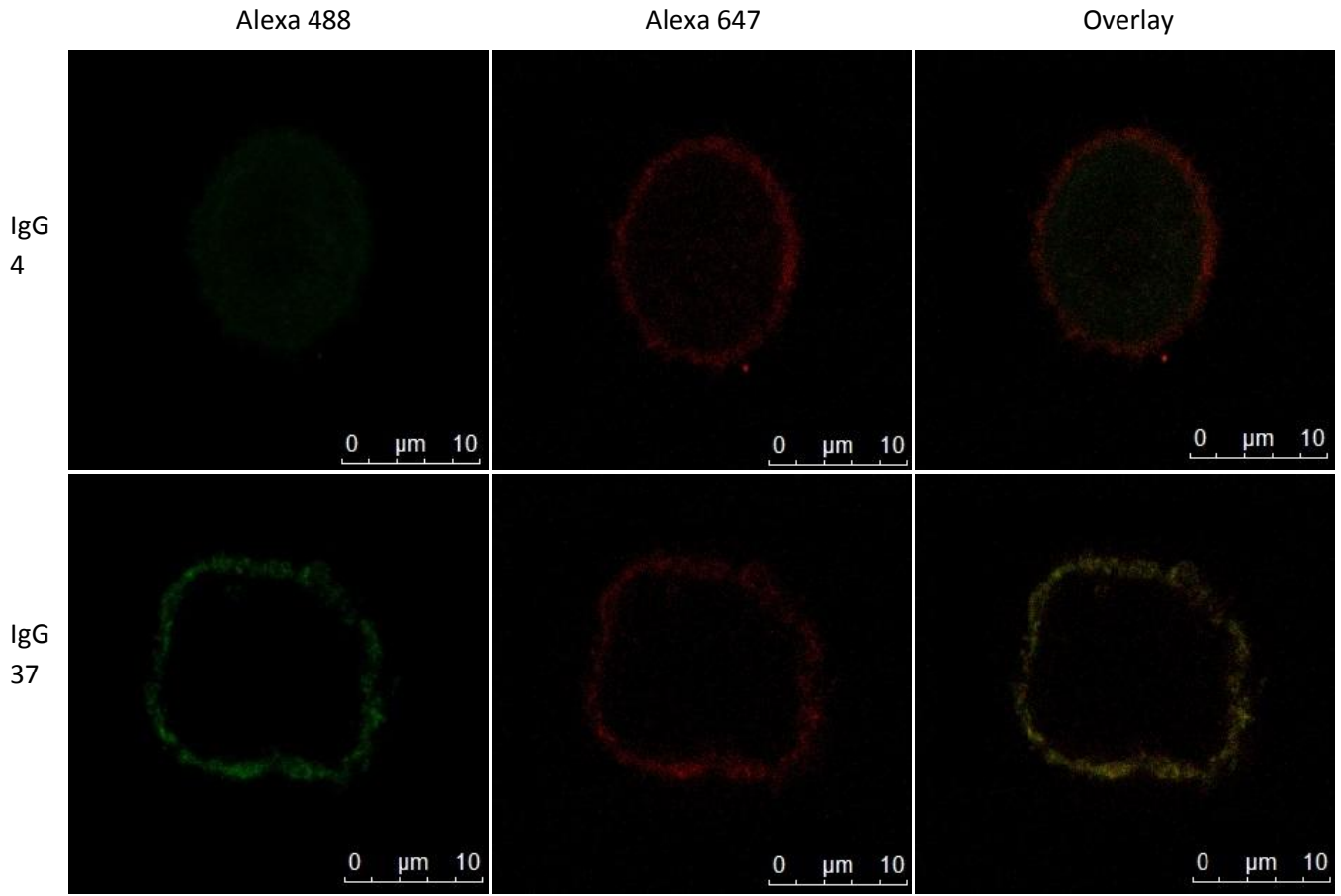


Figure 4.19. IgG controls. DCs cultured with an IgG1,k for 60 minutes at 4 °C and 37 °C. DCs were then stained with HLA-DR Alexa 647 and Goat-anti-mouse Alexa 488 for CD11c or IgG1,k and images were captured with confocal microscopy with a 100x objective. Left to right: Left: Goat-anti-mouse Alexa 488. Middle: Anti-human HLA-DR Alexa 647. Right: Overlay of Alexa 488 and Alexa 647. Top to bottom: Top: IgG1,k 4 °C. Bottom: IgG1,k 37 °C.

An IgG control was included, where DCs were incubated with IgG1,k for 60 minutes at either 4 °C or 37 °C. IgG is not expected to be bound or internalized, and observed in figure 4.19, the goat-anti-mouse Alexa 488 stain is very dim. The HLA-DR Alexa 647 was unexpectedly very dim as well for the two IgG1,k images.

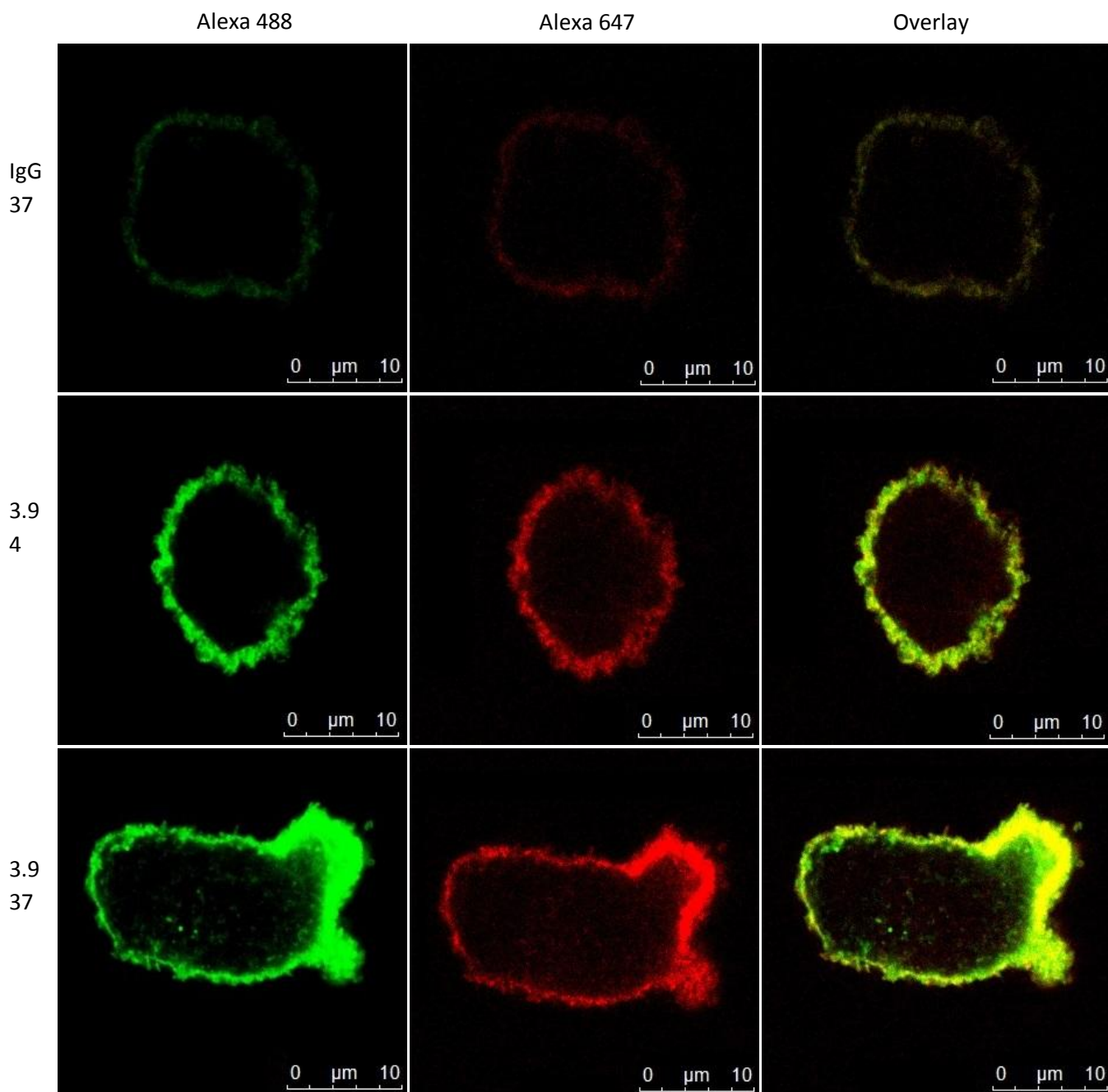


Figure 4.20.1. DCs cultured with CD11c clone 3.9 for 60 minutes at 4 or 37 °C. DCs were then stained with HLA-DR Alexa 647 and Goat-anti-mouse Alexa 488 for CD11c or IgG1,k and images were captured with confocal microscopy with a 100x objective. Left to right: Left: Goat-anti-mouse Alexa 488. Middle: Anti-human HLA-DR Alexa 647. Right: Overlay of Alexa 488 and Alexa 647. Top to bottom: Top: IgG1,k 37 °C. Middle: CD11c 3.9 4 °C. Bottom: CD11c 3.9 37 °C.

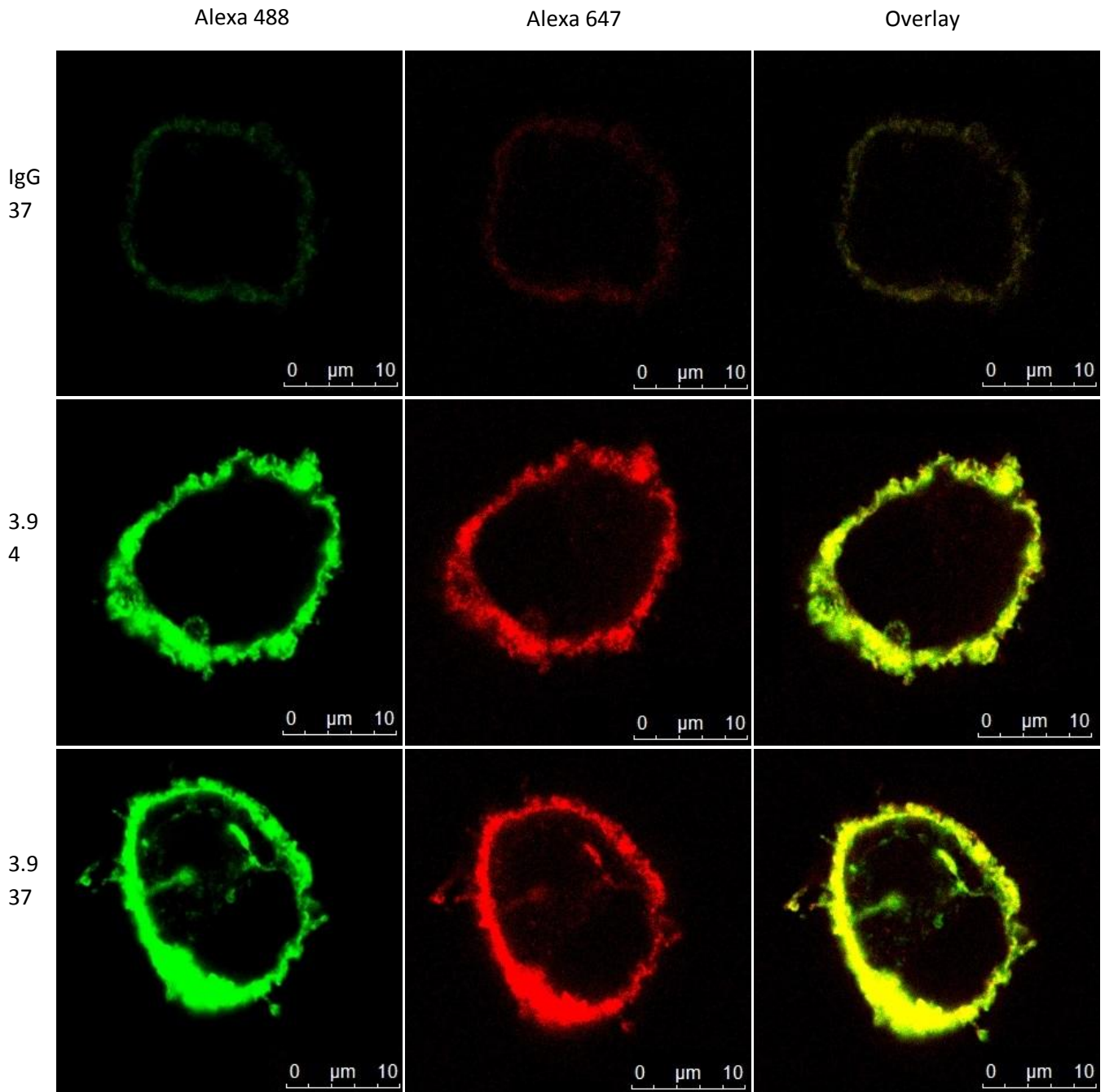


Figure 4.20.2. DCs cultured with CD11c clone 3.9 for 60 minutes at 4 or 37 °C. DCs were then stained with HLA-DR Alexa 647 and Goat-anti-mouse Alexa 488 for CD11c or IgG1,k and images were captured with confocal microscopy with a 100x objective. Left to right: Left: Goat-anti-mouse Alexa 488. Middle: Anti-human HLA-DR Alexa 647. Right: Overlay of Alexa 488 and Alexa 647. Top to bottom: Top: IgG1,k 37 °C. Middle: CD11c 3.9 4 °C. Bottom: CD11c 3.9 37 °C.

Figure 4.20.1 and 4.20.2 illustrates 2 examples of DCs incubated with CD11c antibody clone 3.9 at either 4 °C or 37 °C compared to an IgG control from the same experiment. The stain is very bright and shows no internalization of CD11c 3.9 when incubated at 4 °C, but some internalization is observed at 37 °C. There is some co-localization with internal HLA-DR compartments.

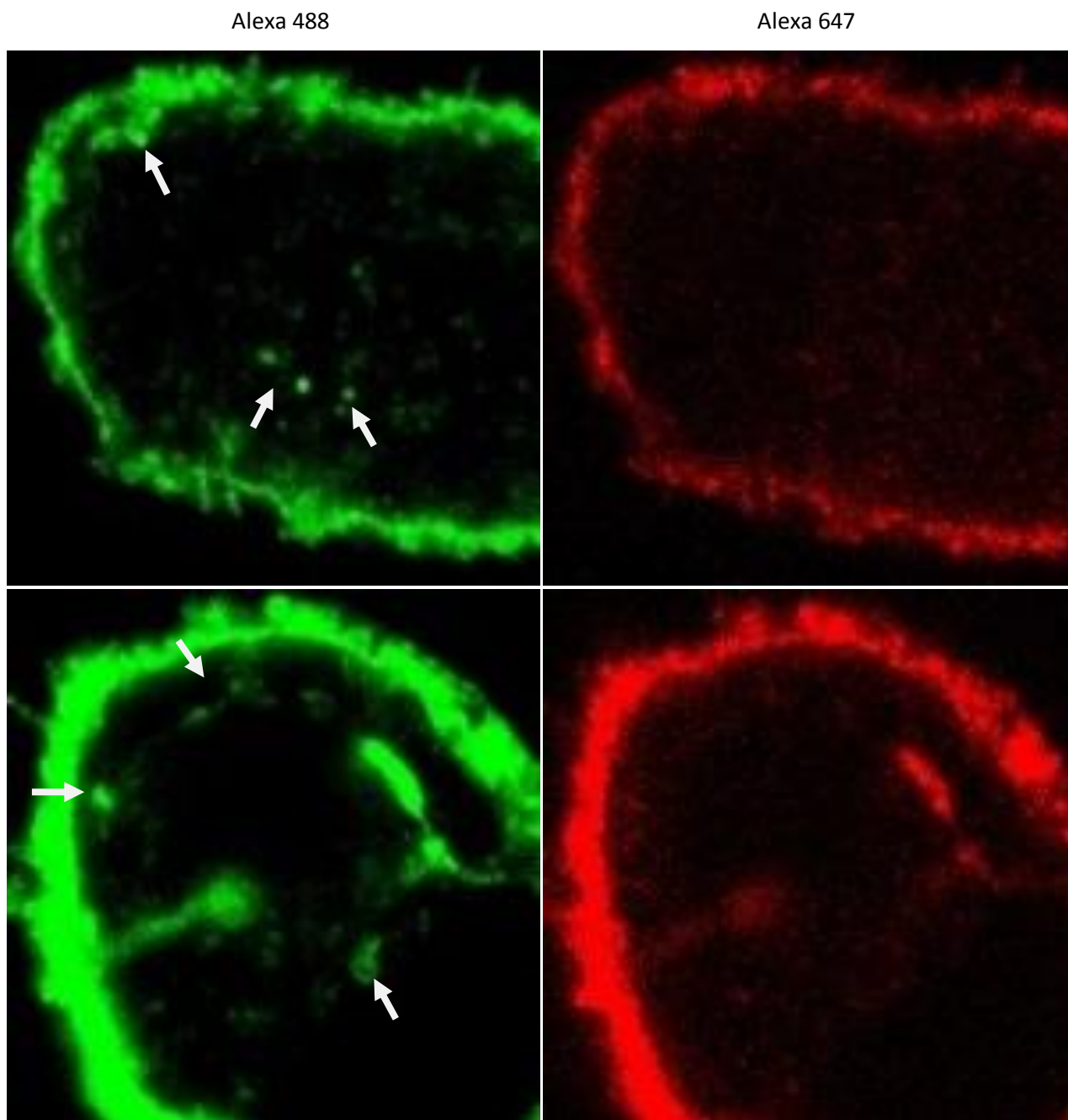


Figure 4.20.3. Close up images of CD11c clone 3.9 incubated for 60 minutes at 37 °C. Left: Goat-anti-mouse Alexa 488. Right: Anti-human HLA-DR Alexa 647. Arrows indicate differences in fluorescence in the two images.

Figure 4.20.3 illustrates a close up image of each of the examples with CD11c clone 3.9 incubated at 37 °C. There are areas that are only visible in the green channel with no co-localization with HLA-DR in the red channel.

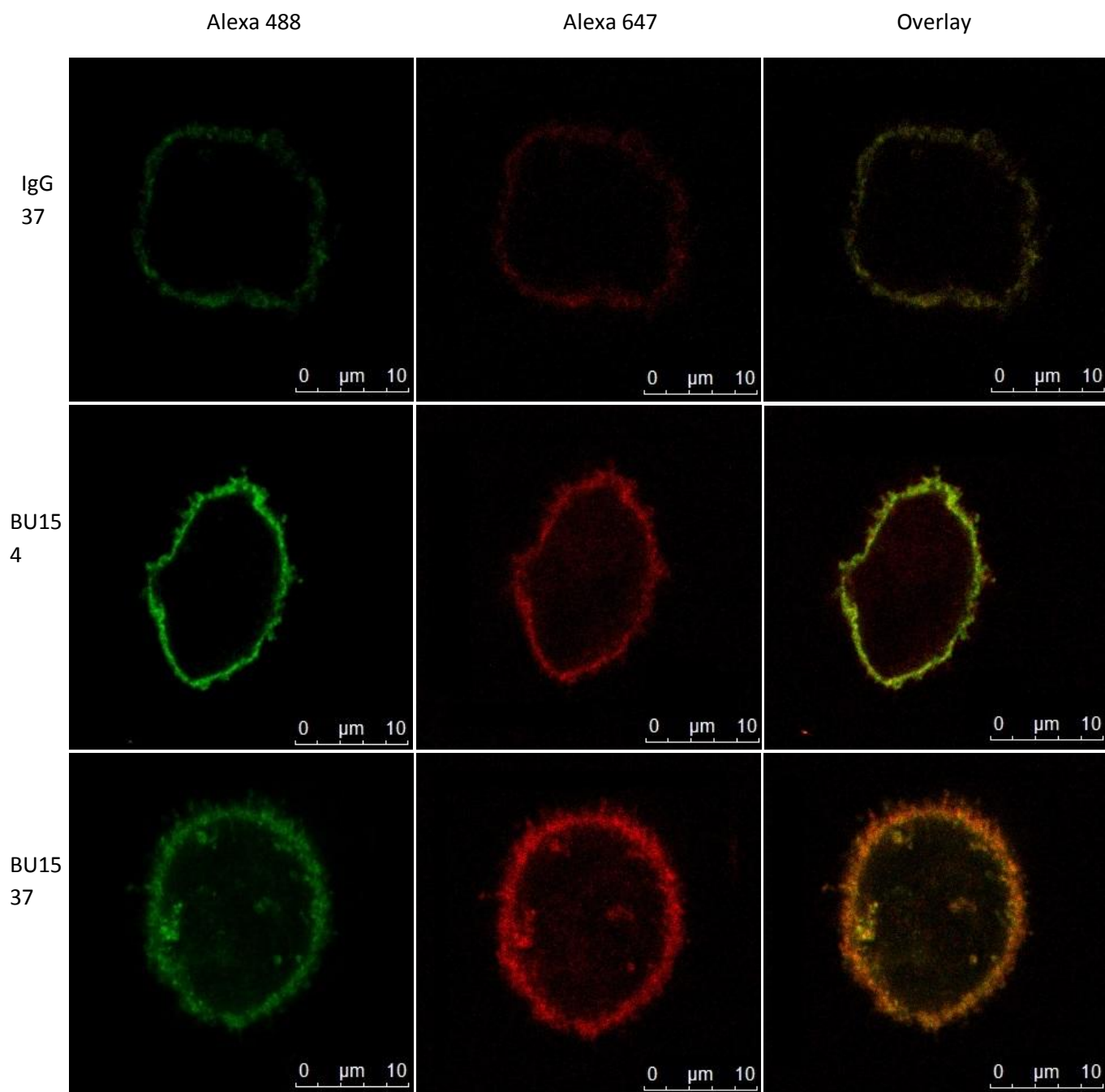


Figure 4.21.1. DCs cultured with CD11c clone BU15 for 60 minutes at 4 or 37 °C. DCs were then stained with HLA-DR Alexa 647 and Goat-anti-mouse Alexa 488 for CD11c or IgG1,k and images were captured with confocal microscopy with a 100x objective. Left to right: Left: Goat-anti-mouse Alexa 488. Middle: Anti-human HLA-DR Alexa 647. Right: Overlay of Alexa 488 and Alexa 647. Top to bottom: Top: IgG1,k 37 °C. Middle: CD11c BU15 4 °C. Bottom: CD11c BU15 37 °C.

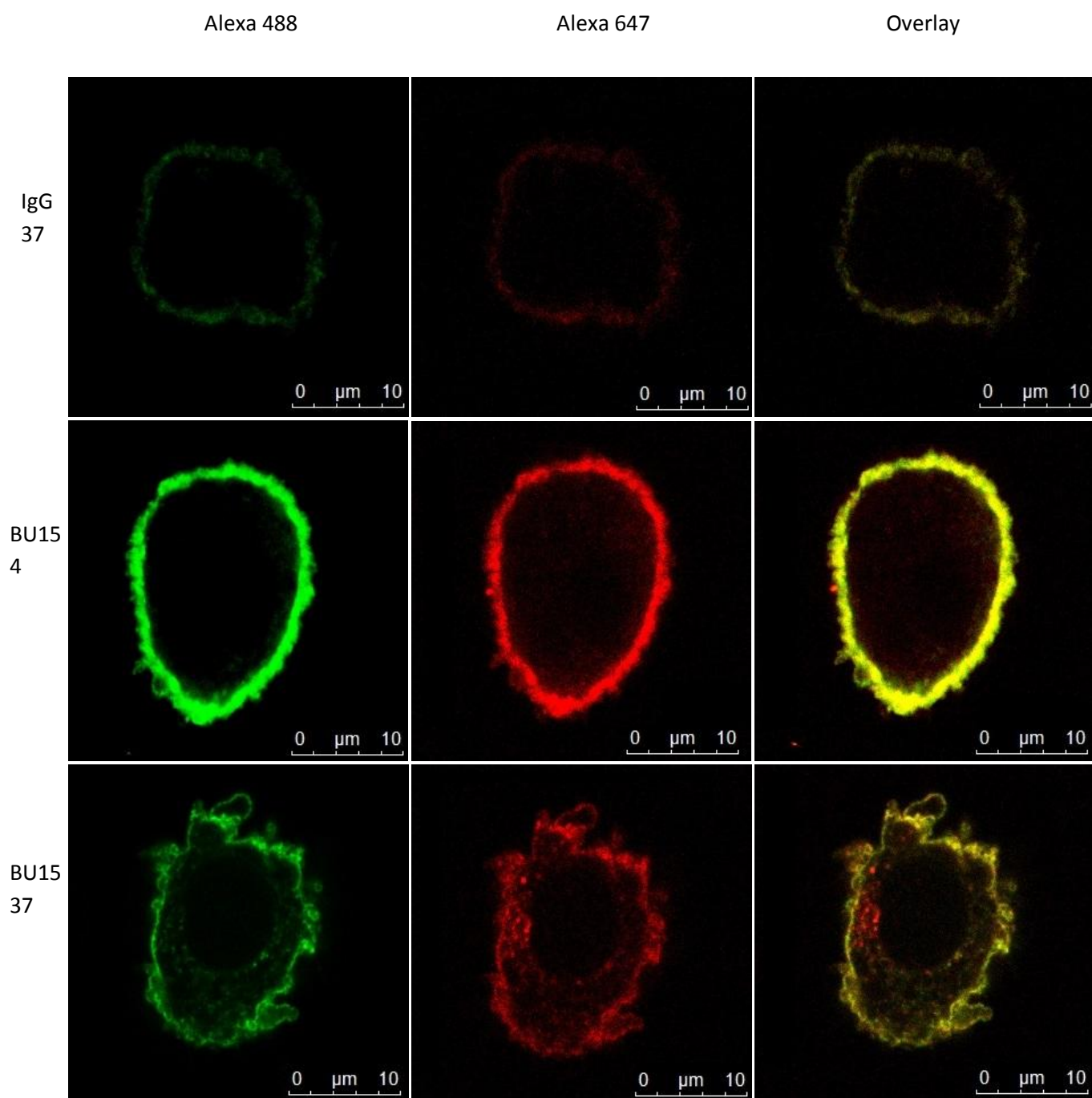


Figure 4.21.2. DCs cultured with CD11c clone BU15 for 60 minutes at 4 or 37 °C. DCs were then stained with HLA-DR Alexa 647 and Goat-anti-mouse Alexa 488 for CD11c or IgG1,k and images were captured with confocal microscopy with a 100x objective. Left to right: Left: Goat-anti-mouse Alexa 488. Middle: Anti-human HLA-DR Alexa 647. Right: Overlay of Alexa 488 and Alexa 647. Top to bottom: Top: IgG1,k 37 °C. Middle: CD11c BU15 4 °C. Bottom: CD11c BU15 37 °C.

Figure 4.21.1 and 4.21.2 illustrates 2 examples of DCs incubated with CD11c antibody clone BU15 at either 4 °C or 37 °C compared to an IgG control. The stain shows no internalization of CD11c BU15 when incubated at 4 °C, and internalization in intracellular compartments is observed at 37 °C. There is some co-localization with internal HLA-DR compartments.

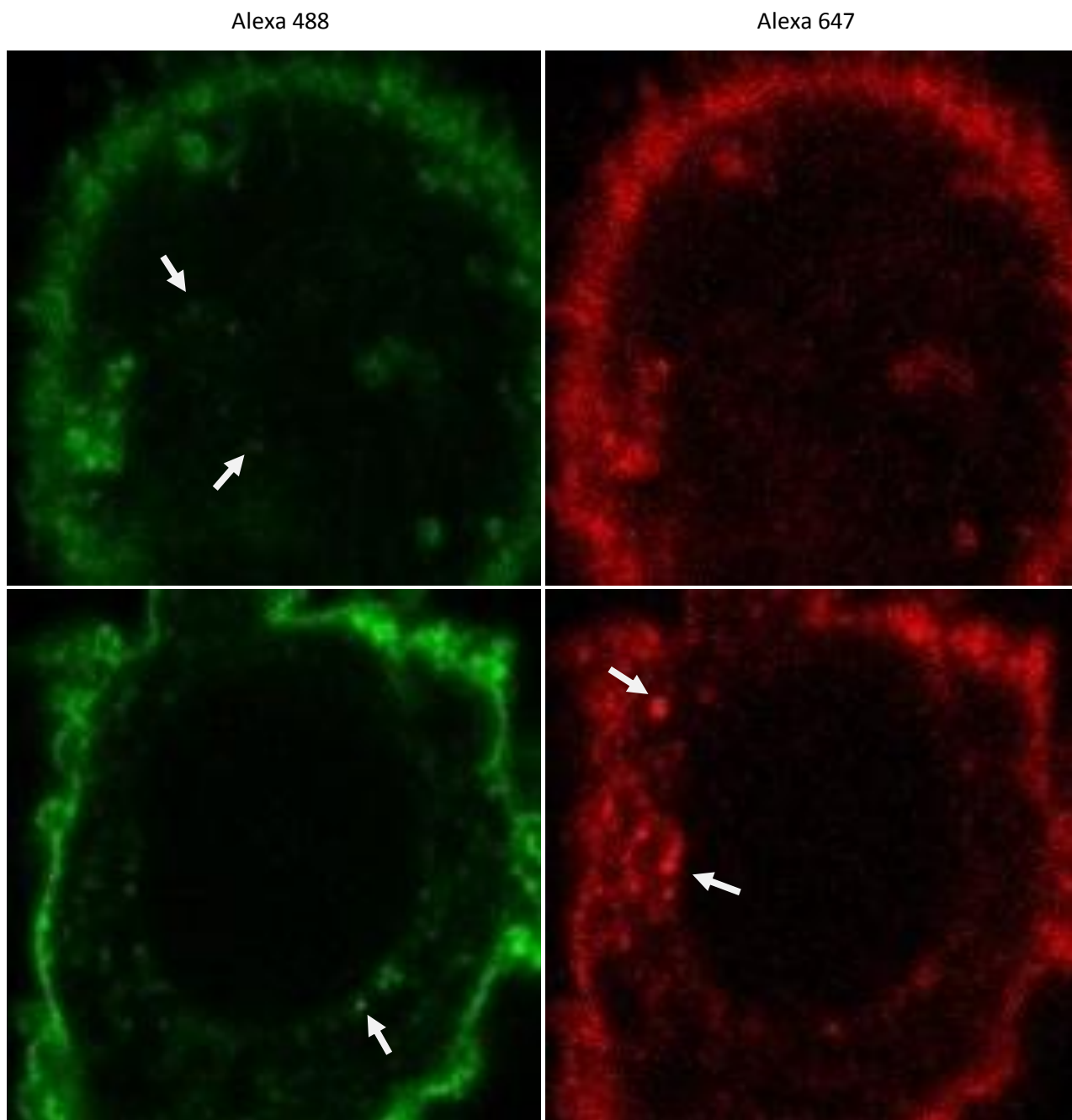


Figure 4.21.3. Close up images of CD11c clone BU15 incubated for 60 minutes at 37 °C. Left: Goat-anti-mouse Alexa 488. Right: Anti-human HLA-DR Alexa 647. Arrows indicate differences in fluorescence in the two images.

Figure 4.21.3 illustrates a close up image of each of the examples with CD11c clone BU15 incubated at 37 °C. There are few areas that are only visible in the green channel with no co-localization in the red channel, and a large area in the left side of the cell that is only visible in the red channel.

4.6.2 Flow cytometric analysis

Internalization was analyzed with flow cytometry to quantitatively determine if the CD11c antibody clones were internalized by the DCs.

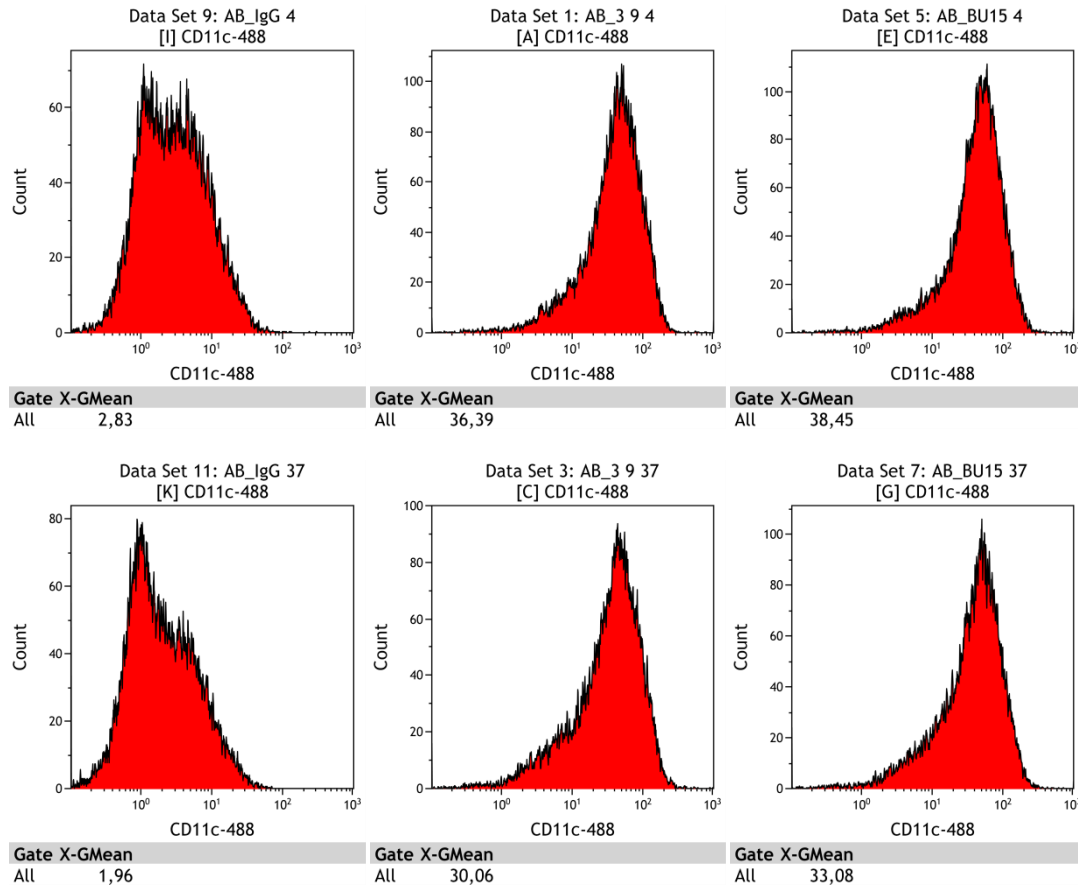


Figure 4.22. Flow cytometric analysis of IgG, CD11c 3.9 and BU15 internalization. Histograms: The y-axis represents the cell count, x-axis represents fluorescence intensity for CD11c antibodies stained with goat-anti-mouse Alexa 488. Raw data and controls for the samples illustrated can be found in appendix 8.2.7.

IgG MFI was subtracted from both CD11c clones, and the percentage of internalization was calculated for each clone from the MFI values for 4 °C and 37 °C incubation. There was a 16,27 % internalization for CD11c clone 3.9, and a 12,63 % internalization for CD11c clone BU15. Calculations can be found in appendix 8.2.7.

4.7 CD11c as an antigen target

4.7.1 Presentation of a CD11c mouse monoclonal antibody to a mouse immunoglobulin specific T cell clone

Due to time constraints, this part of the experiments could not be incorporated in the thesis. Currently, a human CD4⁺ T_H1 cell clone called T18, specific for the kappa chain C_κ⁴⁰⁻⁴⁸ on mice, is being cultured and prepared for experiments with presentation of CD11c to a DC population. The T cell clone was obtained and created by Schjetne et al. from the Institute of Immunology in Oslo, Norway, by isolating T cells from an individual accidentally exposed to mouse Ig in three separate needle injuries. The T18 clone is restricted by HLA-DRB1*0401 (62). PBMCs were isolated from a heterozygous HLA-DRB1*0401/0403 blood donor from Aalborg Sygehus and used to function as antigen-presenting cells for the T18 clone. Presently, the T18 clone is being expanded in co-culture with irradiated antigen-presenting cells in the presence of antigen (polyclonal mouse IgG) and IL-2.

The aim of the ongoing experiment is to investigate whether the two CD11c antibody clones 3.9 and BU15 that are both internalized by DCs will also be presented to the T18 T cell clone.

5 Discussion

It is a very exciting time to research and work with DC vaccines with the current technology available today. Many others are making progress in the field every day. Since the PROVENGE vaccine was FDA approved, researchers all over the world have tried to optimize the vaccine to a more cost-efficient version; instead of culturing the DCs *ex vivo*, create a targeted vaccine that can be given i.v. or i.m. and elicit an immune response *in situ*. Manufacturing such vaccine may eventually turn into an “off the shelf” product that does not need to be personalized for each individual patient, making it easier for healthcare personnel and more economical to treat patients. However, this will probably not apply to all vaccine types due to some variation in some cancer antigens. Imagine the lives that could be saved by discovering vaccines that work against cancer, viral diseases HIV and hepatitis C, bacterial tuberculosis and parasitic malaria.

CD11c has been shown to be a good target for directing antigens to DCs in the mouse. It is clearly of interest to study the human CD11c and if it could also be as useful a target as in the mouse.

These experiments are, to our knowledge, the first reported attempt to investigate maturation and internalization of pure CD11c antibodies in human moDCs.

5.1 Flow cytometry controls

Isotypes generally worked as expected, although the APC-H7 isotype for HLA-DR-APC-H7 had a variance throughout the samples – a common issue with this particular isotype in the Laboratory of Immunology at Aalborg University that could be due to the fact that tandem dyes is known to be sensitive to formaldehyde fixing and extended periods of time in light room or high temperature conditions (63)(64). PE-Cy5 did not display this variance, indicating that this tandem dye might be more stable than APC-H7.

Most samples had a small percentage of lymphocytes, although nearly eliminated in DCs differentiated from CD14⁺ isolated monocytes. The lymphocyte populations could be due to insufficient separation antibodies or columns with a capacity too small.

There were small CD14⁺ populations in the expected DC populations in the pilot experiments. CD14 is used as a monocyte marker, but has been found to be expressed on DCs to a very small extent. As such, it was difficult to conclude if the cells were in fact monocytes or just a subset of DCs that hadn't yet lost their membrane bound CD14. Monocytes were usually present higher on the SSC axis than DCs (see section 4.4.3).

5.2 Confocal microscopy controls

Cultured DCs are known to have a very high autofluorescence in FITC and PE channels (65), so naturally we expected to see some autofluorescence in the unstain images from the 488 channel. However, very little autofluorescence was observed, contrary to what was expected.

The IgG controls turned out as expected – very little binding of the goat-anti-mouse Alexa 488 antibody, and no internalization. However, the low signal from HLA-DR-Alexa 647 was much dimmer than expected, and it was supposed to be just as bright as for the other samples. This could lead to some suspicion whether the signal in the red channel (for Alexa 647) was actually due to a cross reaction between the two

antibodies even after the careful fixing steps performed to avoid this exact issue.

Documented controls for bleed-through were missing in the confocal microscopy experiments, which could have caused some artifacts in the form of co-localization due to cross over from one fluorochrome detected in a wrong channel (e.g. Alexa 488 detected in the 647 channel) (64). However, the fluorochromes are very far apart in the spectrum, and the bleed-through would be minimal.

5.3 Pilot experiments

Pilot experiments were performed to test out some parameters; the monocyte isolation kit and the columns used. Before this, a simple experiment was carried out with two DC populations, one that was stimulated with LPS and one without to get an indication of the expression profiles of the immature and mature populations. The difference between mature and immature DCs varies a lot at the Laboratory for Immunology at Aalborg University. It has been very difficult to obtain consistent and reproducible results, and the difference between the immature and mature DC populations was not the best we have seen in regards to the expression of HLA-DR, CD80 and CD83. CD86 showed a nice separation of mature and immature populations. Microscopy images showed clear differences in maturity with a veiled and dendritic morphology for mature DCs compared to the rounder and less shape shifting immature DCs.

Two different monocyte isolation kits were tested; a negative isolation kit "Monocyte Isolation Kit II" and a positive isolation kit "CD14 isolation kit". The purity of monocytes and DCs differentiated was significantly better for the CD14⁺ kit with very few lymphocytes and debris (see section 4.4.5). However, the DCs matured even when cultured without LPS, which meant that the kit could not be used as it was crucial to be able to differentiate between immature and mature populations in later experiments. The purity of the Monocyte Isolation Kit II in later experiments (see section 4.4.4) was not nearly as great as with the CD14⁺ kit, but the difference between immature and mature populations was clear.

To optimize the Monocyte Isolation Kit II, two different column types were tested to see if it would make a difference in the difference in DC maturation. No difference was observed and purity was approximately the same with a maximum of 2 % lymphocytes which was acceptable (section 4.3.3).

However, lymphocyte percentages increased throughout the experiments, and for some samples the lymphocyte populations totaled about 20 % of the events in the samples. This could be due to the capacity of the columns or that the columns used were old and needed replacing.

5.4 CD11c distribution

In whole blood samples, the monocyte (and DC) populations were positive for CD11c and CD14. In PBMC samples, the same was true, but a slightly CD11c positive population was observed in granulocyte and lymphocyte gates, which was also confirmed in the PBMC samples analyzed on the flow cytometric cell sorter, where a defined population was slightly positive for both HLA-DR and CD11c but not CD14 (see section 4.4.3). Presumably, this population is B-cells due to their small size, location in the lymphocyte gate and them being positive for HLA-DR. It would be interesting to analyze this population further by staining against CD11c, HLA-DR and CD19 to conclude if it is in fact B cells.

In monocytes isolated with the Monocyte Isolation Kit II and CD14 Isolation Kit the results matched those

from whole blood and PBMC samples, where the monocyte population was positive for CD11c, and a very small population slightly positive for CD11c was observed among lymphocytes.

It would be interesting to include a macrophage marker and possibly markers for different granulocytes and natural killer (NK) cells to investigate whether CD11c is expressed on these cells or not.

5.5 Maturation

Neither of the CD11c antibody clones (3.9 and BU15) induced maturation when cultured with DCs in both high and low concentrations (1 and 5 µg/ml). Clone 3.9 seemed to have a very slight effect on the expression of CD86. Clone BU15 even seemed to downregulate the expression of HLA-DR, CD80 and CD83. This was very interesting, since previous research has shown that anti-CD11c can induce maturation in DCs (5).

One could try and increase the concentration to 10 or even 20 µg/ml to see if antibody concentration would yield different results, although it would be reaching very unnatural levels, and the maturation may not be due to the actual antibodies. Another thing could be to culture the DCs with CD11c antibodies for longer than 24 hours, for example 48 hours.

It would seem that if using CD11c as a target for a vaccine, adjuvants (TLR ligands like Poly I:C) would be absolutely vital to include to ensure DC maturation (5).

5.6 Internalization

Internalization of both CD11c clones (3.9 and BU15) was observed in confocal microscopy, and the flow cytometric analysis confirmed a 16,27 % internalization for clone 3.9 and 12,63 % internalization for clone BU15. There is co-localization of HLA-DR and CD11c in the membrane and in some internal compartments. To further investigate which compartments CD11c is processed in, one could investigate and stain for lysosomal-associated membrane protein 1 (LAMP1, found in lysosomal compartments) and Ras-related protein (RAB7, found in endosomal compartments) as well to look for co-localization. LAMP1 co-localization would indicate that CD11c enters into lysosomes and RAB7 co-localization would indicate the CD11c enters into endosomes. If CD11c co-localized with RAB7, this could indicate that CD11c is an optimal target for cross-presentation as antigens processed through RAB7⁺ endosomes is presented on MHC I molecules (66). The HLA-DR-Alexa 647 stain was very weak, and all images had major adjustments in contrast to make the red color show up as intensely as the green Alexa 488. An identical internalization experiment was performed (appendix 8.2.8), but failed due to a too weak HLA-DR-Alexa 647 stain.

5.7 Perspectives

CD11c is expressed on cDCs and to a lesser extent pDCs (23). The response from pDCs will probably not be as high as for cDCs in a vaccine with CD11c as a target, therefore it could be beneficial to target the vaccine to one of the specific pDC markers (CD303 and CD304) for a boost in pDC response.

A question to be asked is: What happens to monocytes and macrophages if they are targeted with a CD11c-

based vaccine? Could there be any adverse effects from antigen presentation on cells other than DCs? The knowledge we are gathering about DC vaccines could possibly be used in reverse to combat allergy and autoimmune diseases as well by giving the vaccine without adjuvants. This would result in immature DCs expressing the vaccine antigen, inducing antigen-specific tolerance (54). CD11c could quite possibly be one of the better options for such “reverse” vaccine, as it does not seem to induce maturation in DCs. The next step would be the investigation of T-cell activation by DCs stimulated with CD11c antibodies and a maturation stimulus, which is a currently ongoing experiment that was not included due to time constraints. The T cell culture and experiment was started mid May and will be finished early to mid June. Cross-presentation is vital for a cytotoxic T-cell response, and therefore it could be interesting to investigate whether anti-CD11c antibodies will also be presented on MHC I. Unfortunately, we have not been able to locate a CD8⁺ T cell clone suitable for this purpose.

This thesis represents the first step towards a human DC vaccine targeting CD11c. When the optimal anti-CD11c antibody has been identified for the purpose, the plan is to use the variable parts of the antibody to construct a human recombinant vaccine that binds to CD11c and contains antigen epitopes and possibly PRR ligands to induce maturation in DCs.

If further experiments prove that CD11c is an exceptionally good target for the purpose of antigen targeting as expected, the end goal is the manufacturing of a human CD11c targeting vaccine for use in the clinic.

6 Conclusion

CD11c is still a very promising target for a future DC vaccine. CD11c antibodies does not induce maturation in DCs, but this can be solved by giving Poly I:C with the vaccine. CD11c antibodies were internalized and some co-localization with HLA-DR compartments was observed.

7 Bibliography

- (1) Kurts C. CD11c: Not merely a murine DC marker, but also a useful vaccination target. *Eur J Immunol* 2008;38(8):2072-2075.
- (2) Ejaz A, Ammann CG. Targeting Viral Antigens to CD11c on Dendritic Cells Induces Retrovirus-Specific T Cell Responses. *PLoS ONE* 2012;7(9):e45102.
- (3) Cheever MA, Higano CS. PROVENGE (Sipuleucel- T) in prostate cancer: the first FDA- approved therapeutic cancer vaccine. *Clinical cancer research : an official journal of the American Association for Cancer Research* 2011;17(11):3520.
- (4) Di Lorenzo G, Ferro M, Buonerba C. Sipuleucel- T (Provenge®) for castration- resistant prostate cancer. *BJU Int* 2012;110(2):E99-E104.
- (5) Cruz LJ, Rosalia RA, Kleinovink JW, Rueda F, Lowik CWGM, Ossendorp F. Targeting nanoparticles to CD40, DEC-205 or CD11c molecules on dendritic cells for efficient CD8.sup.+ T cell response: A comparative study. *J Controlled Release* 2014;192:209.
- (6) Castro FVV, Tutt AL, White AL, Teeling JL, James S, French RR, et al. CD11c provides an effective immunotarget for the generation of both CD4 and CD8 T cell responses. *Eur J Immunol* 2008;38(8):2263.
- (7) Wei H, Wang S, Zhang D, Hou S, Qian W, Li B, et al. Targeted delivery of tumor antigens to activated dendritic cells via CD11c molecules induces potent antitumor immunity in mice. *Clinical cancer research : an official journal of the American Association for Cancer Research* 2009;15(14):4612.
- (8) Clinical Trials. Study record detail: DEC-205/NY-ESO-1 Fusion Protein CDX-1401, Poly ICLC, and IDO1 Inhibitor INCB024360 in Treating Patients With Ovarian, Fallopian Tube, or Primary Peritoneal Cancer in Remission. 2015; Available at: <https://clinicaltrials.gov/ct2/show/NCT02166905?term=cd205&rank=1>.
- (9) Steinman RM, Cohn ZA. Identification of a novel cell type in peripheral lymphoid organs of mice. I. Morphology, quantitation, tissue distribution. *J. Exp. Med.*1973. 137: 1142-1162. *Journal of immunology* (Baltimore, Md.: 1950) 1973;178(1):5.
- (10) Agger R, Andersen V, Leslie G, Aasted B. *Immunologi*. ISBN: 8791319129 2005;4. udgave.
- (11) Banchereau J, Briere F, Caux C, Davoust J, Lebecque S, Liu Y, et al. Immunobiology of Dendritic Cells. *Annu Rev Immunol* 2000;18(1):767-811.
- (12) Fearnley DB, Whyte LF, Carnoutsos SA, Cook AH, Hart DN. Monitoring human blood dendritic cell numbers in normal individuals and in stem cell transplantation. *Blood* 1999;93(2):728.
- (13) Dudek AM, Martin S, Garg AD, Agostinis P. Immature, Semi- Mature, and Fully Mature Dendritic Cells: Toward a DC- Cancer Cells Interface That Augments Anticancer Immunity. *Frontiers in immunology* 2013;4:438.
- (14) Sallusto F, Schaerli P, Loetscher P, Scharniel C, Lenig D, Mackay CR, et al. Rapid and coordinated switch in chemokine receptor expression during dendritic cell maturation. *Eur J Immunol* 1998;28(9):2760.

- (15) Neubert K, Lehmann CHK, Heger L, Baranska A, Staedtler AM, Buchholz VR, et al. Antigen delivery to CD11c+CD8- dendritic cells induces protective immune responses against experimental melanoma in mice in vivo. *Journal of immunology* (Baltimore, Md.: 1950) 2014;192(12):5830.
- (16) Landsverk OJB. MHC II and the endocytic pathway; Regulation by Invariant Chain. 2011.
- (17) Pugholm L. Identification of Target Structures for New Vaccines Specifically Directed at Dendritic Cells. Unpublished.
- (18) Mosmann TR, Sad S. The expanding universe of T-cell subsets: Th1, Th2 and more. *Immunol Today* 1996;17(3):138-146.
- (19) Steinman L. A brief history of TH17, the first major revision in the TH1/ TH2 hypothesis of T cell-mediated tissue damage. *Nat Med* 2007;13(2):139.
- (20) Corthay A. How do Regulatory T Cells Work? *Scand J Immunol* 2009;70(4):326-336.
- (21) Sakaguchi S. Naturally arising CD4+ regulatory t cells for immunologic self- tolerance and negative control of immune responses. *Annu Rev Immunol* 2004;22:531.
- (22) Shortman K, Liu Y. Mouse and human dendritic cell subtypes. *Nature Reviews Immunology* 2002;2(3):151.
- (23) Merad M, Sathe P, Helft J, Miller J, Mortha A. The dendritic cell lineage: ontogeny and function of dendritic cells and their subsets in the steady state and the inflamed setting. *Annu Rev Immunol* 2013;31:563.
- (24) Ziegler-Heitbrock L, Ancuta P, Crowe S, Dalod M, Grau V, Hart DN, et al. Nomenclature of monocytes and dendritic cells in blood. *Blood* 2010;116(16).
- (25) Malissen B, Tamoutounour S, Henri S. The origins and functions of dendritic cells and macrophages in the skin. *Nature Reviews Immunology* 2014;14(6):417.
- (26) NCBI Gene. CD207 CD207 molecule, langerin [*Homo sapiens* (human)]. 2015; Available at: <http://www.ncbi.nlm.nih.gov/gene/50489>.
- (27) Klechevsky E, Morita R, Liu M, Cao Y, Coquery S, Thompson-Snipes L, et al. Functional Specializations of Human Epidermal Langerhans Cells and CD14 + Dermal Dendritic Cells. *Immunity* 2008;29(3):497-510.
- (28) Haniffa M, Shin A, Bigley V, MCGovern N, Teo P, See P, et al. Human Tissues Contain CD141hi Cross-Presenting Dendritic Cells with Functional Homology to Mouse CD103+ Nonlymphoid Dendritic Cells. *Immunity* 2012;37(1):60-73.
- (29) Reizis B, Bunin A, Ghosh HS, Lewis KL, Sisirak V. Plasmacytoid dendritic cells: recent progress and open questions. *Annu Rev Immunol* 2011;29:163.
- (30) Osugi Y, Vuckovic S, Hart DNJ. Myeloid blood CD11c(+) dendritic cells and monocyte- derived dendritic cells differ in their ability to stimulate T lymphocytes. *Blood* 2002;100(8):2858.

- (31) NCBI Gene. HLA-DRB1 major histocompatibility complex, class II, DR beta 1 [*Homo sapiens* (human)]. 2015; Available at: <http://www.ncbi.nlm.nih.gov/gene/3123>.
- (32) NCBI Gene. CD80 CD80 molecule [*Homo sapiens* (human)]. 2015; Available at: <http://www.ncbi.nlm.nih.gov/gene/941>.
- (33) NCBI Gene. CD86 CD86 molecule [*Homo sapiens* (human)]. 2015; Available at: <http://www.ncbi.nlm.nih.gov/gene/942>.
- (34) NCBI Gene. CD40 CD40 molecule, TNF receptor superfamily member 5 [*Homo sapiens* (human)]. 2015; Available at: <http://www.ncbi.nlm.nih.gov/gene/958>.
- (35) Lechmann M, Berchtold S, Steinkasserer A, Hauber J. CD83 on dendritic cells: more than just a marker for maturation. *Trends Immunol* 2002;23(6):273-275.
- (36) NCBI Gene. CD83 CD83 molecule [*Homo sapiens* (human)]. 2015; Available at: <http://www.ncbi.nlm.nih.gov/gene/9308>.
- (37) NCBI Gene. CD1A CD1a molecule [*Homo sapiens* (human)]. 2015; Available at: <http://www.ncbi.nlm.nih.gov/gene/909>.
- (38) Leslie DS, Dascher CC, Cembrola K, Townes MA, Hava DL, Hugendubler LC, et al. Serum lipids regulate dendritic cell CD1 expression and function. *Immunology* 2008;125(3):289-301.
- (39) NCBI Gene. THBD thrombomodulin [*Homo sapiens* (human)]. 2015; Available at: <http://www.ncbi.nlm.nih.gov/gene/7056>.
- (40) NCBI Gene. CLEC4C C-type lectin domain family 4, member C [*Homo sapiens* (human)]. 2015; Available at: <http://www.ncbi.nlm.nih.gov/gene/170482>.
- (41) Riboldi E, Daniele R, Parola C, Inforzato A, Arnold PL, Bosisio D, et al. Human C- type lectin domain family 4, member C (CLEC4C/ BDCA- 2/ CD303) is a receptor for asialo- galactosyl- oligosaccharides. *The Journal of biological chemistry* 2011;286(41):35329.
- (42) NCBI Gene. NRP1 neuropilin 1 [*Homo sapiens* (human)]. 2015; Available at: <http://www.ncbi.nlm.nih.gov/gene/8829>.
- (43) Meyerson HJ, Blidaru G, Edinger A, Osei E, Schweitzer K, Fu P, et al. NRP- 1/ CD304 expression in acute leukemia: a potential marker for minimal residual disease detection in precursor B- cell acute lymphoblastic leukemia. *Am J Clin Pathol* 2012;137(1):39.
- (44) Dzionek A, Fuchs A, Schmidt P, Cremer S, Zysk M, Miltenyi S, et al. BDCA- 2, BDCA- 3, and BDCA- 4: three markers for distinct subsets of dendritic cells in human peripheral blood. *Journal of immunology* (Baltimore, Md.: 1950) 2000;165(11):6037.
- (45) Biolegend. Purified anti-human CD11c Antibody. 2014; Available at: <http://www.biolegend.com/purified-anti-human-cd11c-antibody-564.html>.

- (46) NCBI Gene. ITGAX integrin, alpha X (complement component 3 receptor 4 subunit) [*Homo sapiens* (human)]. 2014; Available at: <http://www.ncbi.nlm.nih.gov/gene/3687>.
- (47) Sadhu C, Ting HJ, Lipsky B, Hensley K, Garcia-martinez L, Simon SI, et al. CD11c/CD18: novel ligands and a role in delayed- type hypersensitivity. *J Leukoc Biol* 2007;81(6):1395-1403.
- (48) Vorup-Jensen T, Chi L, Gjelstrup LC, Jensen UB, Jewett CA, Xie C, et al. Binding between the Integrin $\alpha X\beta 2$ (CD11c/ CD18) and Heparin. *J Biol Chem* 2007;282(42):30869-30877.
- (49) Nham S. Characteristics of Fibrinogen Binding to the Domain of CD11c, an α Subunit of p150,95. *Biochem Biophys Res Commun* 1999;264(3):630-634.
- (50) Vorup-Jensen T, Ostermeier C, Shimaoka M, Hommel U, Springer TA. Structure and Allosteric Regulation of the $\alpha X\beta 2$ Integrin I Domain. *Proc Natl Acad Sci U S A* 2003;100(4):1873-1878.
- (51) Pugholm L. Personal correspondence.
- (52) Hsu F, Benike C, Fagnoni F, Liles T, Czerwinski D, Taidi B, et al. Vaccination of patients with B-cell lymphoma using autologous antigen-pulsed dendritic cells. *Nat Med*. 1996 Jan;2(1):52-8. 1996.
- (53) Clinical Trials. *ClinicalTrials.gov is a registry and results database of publicly and privately supported clinical studies of human participants conducted around the world..* 2015; Available at: www.clinicaltrials.gov.
- (54) Palucka K, Banchereau J. Dendritic- Cell- Based Therapeutic Cancer Vaccines. *Immunity* 2013;39(1):38.
- (55) Palucka K, Banchereau J, Mellman I. Designing Vaccines Based on Biology of Human Dendritic Cell Subsets. *Immunity* 2010;33(4):464-478.
- (56) Kevin Evel-Kabler, Si-Yi Chen. Dendritic Cell- Based Tumor Vaccines and Antigen Presentation Attenuators. *Molecular Therapy* 2006;13(5):850.
- (57) Chatterjee B, Smed-Sørensen A, Cohn L, Chalouni C, Vandlen R, Lee B, et al. Internalization and endosomal degradation of receptor- bound antigens regulate the efficiency of cross presentation by human dendritic cells. *Blood* 2012;120(10):2011.
- (58) Faculty of Medicine and Dentistry, University of Alberta, Canada. What is flow cytometry? 2015; Available at: <http://flowcytometry.med.ualberta.ca/>.
- (59) Brown M, Wtttwer C. Flow cytometry: Principles and clinical applications in hematology.(Beckman Conference). *Clin Chem* 2000;46(8):1221.
- (60) eBioscience. Isotype Conrols: What, Why and When? 2012; Available at: <http://info.ebioscience.com/bid/101628/Isotype-Controls-What-Why-and-When>.
- (61) Olympus FluoView Resource Center. Introduction to confocal microscopy. 2009; Available at: <http://www.olympusfluoview.com/theory/confocalintro.html>.

- (62) Schjetne KW, Thompson KM, Aarvak T, Fleckenstein B, Sollid LM, Bogen B. A mouse C kappa-specific T cell clone indicates that DC- SIGN is an efficient target for antibody- mediated delivery of T cell epitopes for MHC class II presentation. *Int Immunol* 2002;14(12):1423.
- (63) BD Biosciences. Selecting reagents for multi-color flow cytometry. 2012; Available at: http://web.mit.edu/flowcytometry/www/Becton%20Dickinson%20Multicolor_AppNote.pdf.
- (64) Olympus FluoView Resource Center. Spectral bleed-through artifacts in confocal microscopy. 2009; Available at: <http://www.olympusconfocal.com/theory/bleedthrough.html>.
- (65) Ni K, Helen CO. Improved FACS analysis confirms generation of immature dendritic cells in long-term stromal-dependent spleen cultures. *Immunol Cell Biol* 2000;78(3):196.
- (66) Shen K, Song Y, Chen I, Leng C, Chen H, Li H, et al. Molecular mechanisms of TLR2-mediated antigen cross-presentation in dendritic cells. *Journal of immunology (Baltimore, Md.: 1950)* 2014;192(9):4233.
- (67) Berntsen A, Geertsen P, Svane I, et al. Therapeutic Dendritic Cell Vaccination of Patients with Renal Cell Carcinoma. *European Urology* 2006;50(1);43.
- (68) RCSB Protein Data Bank. Crystal structure of the alpha-X beta2 integrin I domain, 1N3Y. 2011; Available at: <http://www.pdb.org/pdb/explore/explore.do?structureId=1n3y>
- (69) BD Biosciences. Fluorochrome Spectrum Viewer. 2015; Available at: <http://www.bdbiosciences.com/us/s/spectrumviewer>